(2)

Office of Naval Research
Contract N00014-85-K-0624

Final Report

CHANGES IN ULTRASONIC PULSE SHAPES DUE TO NONLINEAR PROCESSES

by

W. G. Mayer, J. Wolf, and T. D. K. Ngoc.

Walter G. Mayer
Principal Investigator
Department of Physics
Georgetown University
Washington, DC 20057

July 1988

UNCLASSIFIED
SECURITY CLASSIFICATION OF THIS PAGE

REPORT DOCUMENTATION PAGE

Form Approved OMB No. 0704-0188

1a REPORT SECURITY CLASSIFICATION: UNCLASSIFIED	1b RESTRICTIVE MARKINGS
2a SECURITY CLASSIFICATION AUTHORITY	3 DISTRIBUTION / AVAILABILITY OF REPORT: Approved for public release: distribution unlimited
2b DECLASSIFICATION / DOWNGRADING SCHEDULE	
4 PERFORMING ORGANIZATION REPORT NUMBER(S)	5 MONITORING ORGANIZATION REPORT NUMBER(S)
6a NAME OF PERFORMING ORGANIZATION: Georgetown University; 6b OFFICE SYMBOL (If applicable)	7a NAME OF MONITORING ORGANIZATION: Office of Naval Research
6c ADDRESS (City, State, and ZIP Code): Physics Dept., Georgetown University, Washington, DC 20057	7b ADDRESS (City, State, and ZIP Code): Physics Division, Code 1112, Arlington, VA 22217-5000
8a NAME OF FUNDING / SPONSORING ORGANIZATION; 8b OFFICE SYMBOL (If applicable)	9 PROCUREMENT INSTRUMENT IDENTIFICATION NUMBER: N00014-85-K-0624
8c ADDRESS (City, State, and ZIP Code)	10 SOURCE OF FUNDING NUMBERS

PROGRAM ELEMENT NO.	PROJECT NO.	TASK NO.	WORK UNIT ACCESSION NO.
61153N	4126942		

11 TITLE (Include Security Classification): Changes in Ultrasonic Pulse Shapes due to Nonlinear Processes

12 PERSONAL AUTHOR(S): W. G. Mayer, J. Wolf, and T. D. K. Ngoc

13a TYPE OF REPORT	13b TIME COVERED	14 DATE OF REPORT (Year, Month, Day)	15 PAGE COUNT
Final Report	FROM 850801 TO 880731	880731	88

16 SUPPLEMENTARY NOTATION

17 COSATI CODES			18 SUBJECT TERMS (Continue on reverse if necessary and identify by block number)
FIELD	GROUP	SUB-GROUP	
20	01		ultrasonic pulses; acoustooptics; nonlinearities reflection.

19 ABSTRACT (Continue on reverse if necessary and identify by block number)

Acousto-optic interaction theory is applied to ultrasonic pulses in order to determine pulse parameters from the light diffraction pattern produced by the pulses. Experiments are described to show how pulse shapes change when propagation is in a nonlinear liquid. It is shown that pure electronic determinations of pulse shapes do not describe all the changes accurately whenever the probe response is not known exactly. Use of present method is able to eliminate this problem. Examples of pulse progation as investigated by acousto-optic method are given and evaluated.

20 DISTRIBUTION / AVAILABILITY OF ABSTRACT	21 ABSTRACT SECURITY CLASSIFICATION
☒ UNCLASSIFIED/UNLIMITED ☐ SAME AS RPT. ☐ DTIC USERS	UNCLASSIFIED

22a NAME OF RESPONSIBLE INDIVIDUAL	22b TELEPHONE (Include Area Code)	22c OFFICE SYMBOL
L. E. Hargrove, ONR Physics Division	(202) 696-4221	ONR Code 1112

DD Form 1473, JUN 86 — Previous editions are obsolete. — SECURITY CLASSIFICATION OF THIS PAGE

UNCLASSIFIED

SUMMARY

Background Information

The work described in this report was performed during the last three years in the Ultrasonics Laboratory of the Georgetown University Physics Department. Prior to that period the activities in this laboratory were concerned with ONR-sponsored work on reflection and transmission of continuous waves bounded beams at liquid solid half-space boundaries and solid plates.

At the conclusion of the previous work it had become evident that a great number of aspects of seemingly simple processes of reflection/transmission were unknown or unclear when ultrasonic pulses were used instead of continuous waves. Many of these new aspects were investigated in the course of the present contract and the results are included in this report.

Work Performed and Results

Properties of ultrasonic waves traveling in a liquid have been examined for many years and all important characteristics of continuous infinite plane waves have been studied. However, real ultrasonic signals are never infinite plane waves and rarely are they truly continuous; most ultrasonic work is done by using either pulsed ultrasound or bounded beam (spatially confined and having directivity) signals. Existing plane-wave theories cannot be applied and a new approach was needed to investigate theoretically and experimentally the various problems of ultrasonic pulse propagation and pulse characteristics.

This laboratory has had extensive experience with experimental techniques using acousto-optic interactions (AOI), both in the linear and nonlinear regimes of continuous ultrasonic waves. This AOI method is used to obtain definitive information about important sound field parameters without having to disturb the acoustic field - which is the case when a probe or pickup transducer is used to intercept the signal. The AOI technique is noninvasive.

Moreover, the elimination of a pickup transducer probe also eliminates the errors in signal analysis introduced by any probe transducer's inability to transfer precisely the shape of the vibrational pulse it intercepts in the liquid to an identical electronic signal. Use of the AOI method can yield a true description of the actual shape of the ultrasonic wave as it exists in the liquid.

With this great advantage of the noninvasive AOI method over electronic signal analysis techniques, it was evident that the method should be applied to investigate ultrasonic pulses and their propagation characteristics.

Unfortunately, no complete theory of AOI for ultrasonic pulses existed and no optical system with the required frequency resolution had been constructed. Both problems were solved while the present Contract was in effect.

a) Basic Theory

In the AOI method, the light diffraction pattern produced by the ultrasonic continuous wave yields a measure of the three c.w. signal parameters:

the ultrasonic frequency,

the amplitude,

the harmonic content due to nonlinear processes.

If one measures the light diffraction fringe spacing, light intensity distribution, and order symmetry, respectively, one has determined the three parameters which describe the ultrasonic wave.

If, however, the signal is a series of ultrasonic pulses, the resulting AOI diffraction pattern distribution and shape is determined by

the ultrasonic frequency of the pulse,

the pulse repetition frequency,

the number of bursts in the pulse,

the maximum pulse envelope amplitude,

the pulse rise and decay history,
the harmonic content due to nonlinear processes,
the number of pulses interacting with the light.

In order to use the AOI technique to determine pulse characteristics, the contribution of any of above parameters to the shape of the diffraction pattern must be known.

The theory which was developed to solve this problem is based on the fact that every repetitive waveform can be described in terms of a Fourier frequency spectrum. The lowest frequency component for a sequence of pulses is the pulse repetition rate and all other frequencies in the Fourier spectrum are multiples of the repetition frequency; their respective amplitudes are determined by the magnitudes of the parameters listed above.

After the frequency components for a given pulse sequence are found, their individual contributions to the light fiffraction pattern must be uniquely determined. An analytically accurate theory was developed for this, first and higher order approximations were derived and a code was prepared which is readily usable on a Personal Computer.

Using the results of this theoretical work allows one

1) to calculate the exact shape of the light diffraction pattern produced by any sequence of ultrasonic pulses,
2) to relate any change in the various pulse parameters to changes in the optical pattern produced by the pulses without ever having to base the pulse shape analysis on probe-generated electronic signals,
3) to relate the analysis of an electronically measured pulse shape (probe output) and the acousto-optically evaluated shape of the same pulse to show how much error is introduced by a probe.

b) Experimental Verification

In order to verify this theory a unique arrangement had to be constructed before appropriate experiments could be conducted. AOI experimental setups for continuous waves usually accomodate an optical path length of less than 5 meters which is sufficient to resolve diffraction patterns produced by ultrasonic waves in the low MHz range. These setups usually fail to resolve the pattern when the ultrasonic frequency is below 1 MHz.

As was pointed out above, the lowest frequency component in a sequence of pulses is the repetition frequency. Since it can be orders of magnitude lower than the low-MHz pulse modulation frequency, a much improved system had to be designed to resolve these low frequency component contributions to the expected light diffraction pattern.

The present version of the facility has an optical path length of more than 20 meters, uses spherical mirrors and matched cylindrical lenses, and is capable of resolving diffraction orders produced by frequencies as low as 50 kHz. It is housed in a special room in which temperature fluctuations are eliminated as much as possible and where no other activities take place while an experiment is conducted. Data acquisition is fully automated and the whole arrangement is controlled from a PC which is located in an adjacent room.

The system was then used to experimentally verify the important results of the theoretical analysis concerning the optical signature of the AOI for pulses, particularly the more obvious and drastic changes pulses may experience in the course of propagation in a nonlinear medium or during reflection or transmission at boundaries.

Of particular interest were changes in pulse characteristics and their detectability by means of the AOI technique, including variations in the initially set conditions of pulse shape like

pulse length, amplitude, repetition frequency, duty cycle, and modulation frequency,

as well as pulse characteristics changes occurring during propagation like

frequency content changes due to nonlinearities, reflections, transmissions through solid plates and excitation of resonant modes in solid plates.

Two other interesting topics were considered in the course of the experimental investigations which merit special mention. The first one concerns the difference between phase velocity and group velocity of a pulse traveling in a solid plate. It was found that there are conditions where the propagation direction of the group velocity is opposite to that of the phase velocity. The other topic concerns the interaction of plate vibrations, created by the impinging pulse, with the pulse iself such that certain frequency component of the pulse may be filtered out, making the reflected or transmitted ultrasonic pulse quite different from the initial pulse.

Structure of Report

This Report provides an overview of theory and experiments related to the determination of the shape, form, frequency spectrum and other important properties of ultrasonic pulses traveling in water.

No electronic probes are used in the experiments thus the determination of the parameters is noninvasive.

The results are obtained by using the theory of light diffraction by pulsed ultrasonic waves, which was developed in this Laboratory, and by making use of a specially built experimental setup whose design is based on the dictates of the theory as well as on the experimental conditions usually encountered in work with low-MHz ultrasonic pulses and repetition rates starting slightly above the audible range.

Details of the theoretical and experimental investigations mentioned in this Summary are listed in this Report as follows.

Section 1 is concerned with the theory light diffraction by ultrasonic pulses, the computational techniques, and the basic

experimental, noninvasive determination of the acousto-optic signature of pulses traveling in water.

Section 2 describes in detail the experimental facilitiy, including the optical, electronic, and computational arrangements. The experimental procedure and data evaluation as well as transducer response determination are discussed.

Section 3 contains derivations and results applicable to acousto-optic processes occurring during propagation, reflection, and transmission of ultrasonic pulses in nonlinear media.

Section 4 discusses some of the results which were obtained as a conseuquence of the nonlinear propagation investigation listed in Section 3, including negative group velocities of Lamb modes and the use of solid plates in liquids as spectral filters for high-amplitude pulses.

Some of the text, equations, and figures presented in this Report were taken directly from publications which were prepared under ONR sponsorship of the present Contract. A complete list of titles, authors, and other identifying information of these publications is appended to this report.

Section 1

DIFFRACTION OF LIGHT BY ULTRASONIC WAVES

This section presents the highlights of the theory of light diffraction by ultrasonic pulses, describing how the structure of light patterns produced by pulsed ultrasonic waves can be used to make a comparison with the actual parameters of the pulses as they travel in the liquid medium. General features of measured diffraction patterns are highlighted and a description is given of a numerical model to predict the structure of diffraction patterns. Using the model, comparisons can be made between theoretical and experimental results.

The various theories of acousto-optic interactions have their origins in the standard Raman-Nath theory which was developed about 50 years ago. Most adaptations condidered sound beams which were continuous waves and contained a single frequency, or possibly some amounts of higher harmonics caused by propagation in nonlinear media.

But with the advent of the leaser as a true monochromatic light source it became possible to consider much higher resolution requirements, and the possibilities of investigating multi-frequency ultrasonic signals became realities. To this end, Hargrove [1] derived a theoretical expression to describe diffraction of Gaussian light beams by arbitrary periodic acoustic waves. He solved his expression within the Raman-Nath conditions and illustrated the difference of light diffraction by Gaussian rather than plane light beams. Zitter [2] used Hargrove's expression in a study of light diffraction by short ultrasonic pulses. Häusler et al. [3] demonstrated a qualitative agreement with the work of Zitter by experimentally producing structured diffraction patterns from pulsed ultrasonic waves.

The approach used here resulted in a general theory to describe light diffraction, within the Raman-Nath regime, by pulsed ultrasonic waves. This theory assumes a plane wave opti-

cal beam incident normal to the acoustic wave propagation direction in the medium. As will be shown in a comparison between theory and experiment, the plane wave approximation is sufficient for the purpose of this study.

Theoretical Procedure

The theoretical procedure is based on the same physical principles as was used by Raman and Nath, however, instead of starting with a pure sinusoidal ultrasonic wave, a periodic train of ultrasonic pulses with all of their frequency components is considered [4] to interact with monochromatic light. A typical pulse sequence is shown in Fig. 1-1. The pulse has a repetition frequency f_p and a center modulation frequency f_o, (for comparison consider f_o to be equal to the continuous wave frequency). Harmonic analysis can be performed on these pulse shapes since they are periodic in time. This pulse shape is represented by the Fourier expansion

$$v(\alpha) = \sum_{n=1}^{\infty} v_n \sin(n\alpha_p + \beta_n) \qquad (1\text{-}1)$$

with the definitions:

$v_n = a_n v$

$\alpha_p = w_p t - k_p x$

$w_p = 2\pi f_p$

$k_p = 2\pi/\lambda_p$

λ_p = pulse length in the medium.

The values a_n and β_n are the amplitude and phase of the n^{th} Fourier component of the pulse. The definition of v, the Raman-Nath parameter, is the same as that for continuous waves. Above expression completely defines any periodic pulse shape.

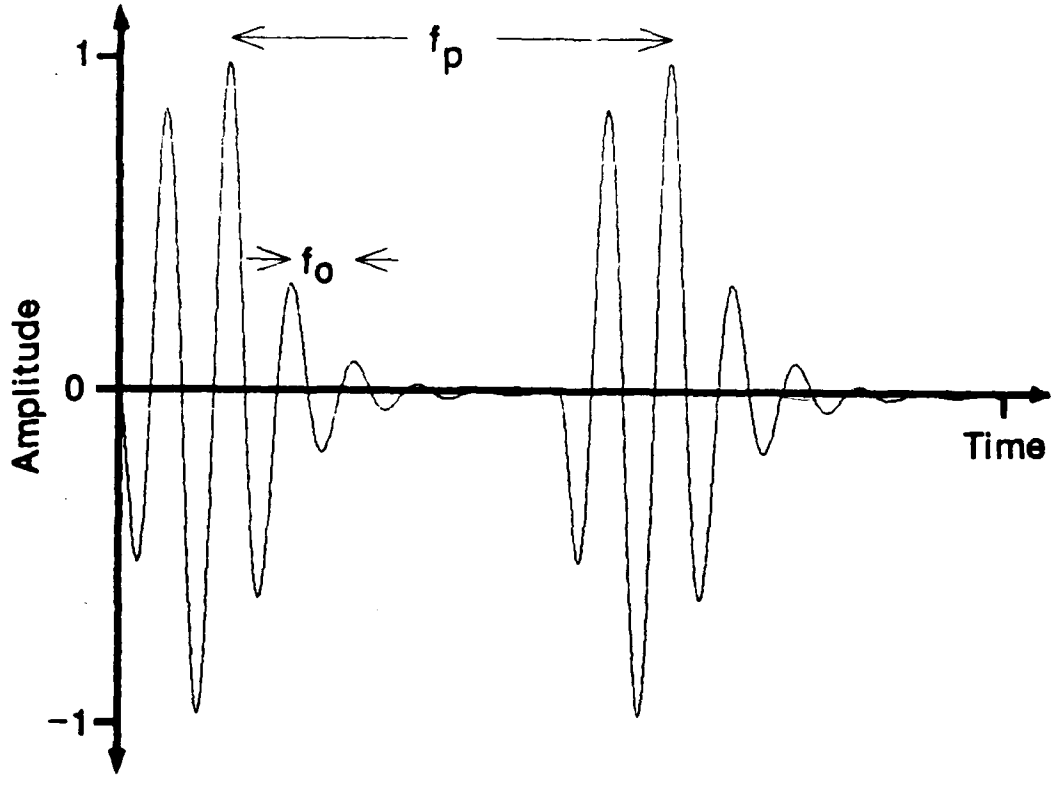

Fig. 1-1. Typical pulse sequence.

Following the same procedure as is employed in the continuous wave case, one substitutes this expression into the standard diffraction integral, performs the integration and takes the square of the real part. However, there is a more complex time dependence introduced by the pulse Fourier spectrum. To obtain the measured response of a photodetector, the intensity expression has to be time averaged over an interval τ which is long compared to the optical period, but short compared to the pulse repetition period, that is

$$w \gg 2\pi/\tau \gg w_p.$$

A restriction on the size of the light window, illuminating the ultrasonic beam, follows from restricting the intensity expression to discrete, fully resolved diffraction patterns. The resulting inequality,

$$2\pi l \gg \lambda_p, \tag{1-2}$$

limits the minimum number of ultrasonic pulses interacting with the light beam at any one time. It is shown in the following sections that this relation establishes the spectral resolution of the experimental apparatus. Observing this restriction provides the light intensity distribution of the diffraction pattern

$$I(\theta) = \sum_{m=-\infty}^{\infty} (\sin\Omega_m/\Omega_m)^2 \, I_m \tag{1-3}$$

where:

$$\Omega_m = (k\sin\theta - mK_p),$$

$$I_m = | \Phi_m |^2,$$

$$\Phi_m = \sum_{r_2=-\infty}^{\infty} \cdots \sum_{r_n=-\infty}^{\infty} J_{r1(m)}(v_1)\cdots J_{rn}(v_n)\cdots$$

$$\cdot\exp\{i[r_1(m)\beta_1 + \cdots + r_n\beta_n + \cdots]\}, \tag{1-4}$$

$$r_1(m) = m - 2r_2 - \cdots - nr_n - \cdots.$$

The expression for $I(\Theta)$ represents a set of discrete diffraction orders each with a spatial form described by the $(\sin\Omega_m/\Omega_m)^2$ term that is maximum at $\Omega_m = 0$ which infers the result

$$\sin\Theta_m = \pm m \lambda/\Lambda_p. \tag{1-5}$$

This result indicates that the diffraction angle is determined by the pulse length in the medium and the light wavelength λ.

The individual I_m cannot be derived exactly from Eq. (1-4). However, since the Bessel functions converge rapidly, the equation can be factored into a set of approximate expressions. If the v_n are assumed small then, to a first approximation, one finds that

$$I_0 = \left| \prod_{n=1}^{\infty} J_0(v_n) \right|^2 \tag{1-6}$$

and

$$I_{\pm m} = \left| J_{\pm 1}(v_m)\ e^{\pm i\beta m} \prod_{n<>m}^{\infty} J_0(v_n) \right|^2 \tag{1-7}$$

where π indicates the product over n. The intensity distribution is symmetric about $m = 0$. For small ultrasonic pulse amplitudes $I_0 \approx 1$ and

$$I_{\pm m} \approx v_m^2/4. \tag{1-8}$$

This equation contains one important result, namely:

To a first approximation, the intensity in the individual diffraction orders provides a direct measure of the pulse amplitude spectrum.

In general, the diffraction pattern is not symmetric. This happens when the pulse peak amplitude is large or the initial pulse spectrum has higher harmonic terms in it. This can be illustrated with asecond order approximation solution, given by

$$I_{\pm m} = \Big| J_{\pm 1}(v_m)\, e^{\pm i\beta m} \prod_{\substack{n=1 \\ n<>m}}^{\infty} J_0(v_n) + J_2(v_{m/2})\, e^{\pm 2\beta m/2} \prod_{\substack{k=1 \\ k<>m/2}}^{\infty} J_0(v_k)$$

$$+ \sum_{\substack{n=1 \\ 2n<m}}^{\infty} \{J_{\pm 1}(v_n)\, J_{\pm 1}(v_{m-n})\, e^{\pm i(\beta n + \beta m - n)} \prod_{\substack{k=1 \\ k<>n,m-n}}^{\infty} J_0(v_k)\}$$

$$+ \sum_{n=1}^{\infty} \{J_{-+1}(v_n)\, J_{\pm 1}(v_{n+m})\, e^{\pm i(\beta n+m - \beta n)} \prod_{\substack{k=1 \\ k<>n,n+m}}^{\infty} J_0(v_k)\}\Big|^2 \qquad (1\text{-}9)$$

with the notational convention that all terms with noninteger summation indices vanish. The first term is simply Eq. (1-7). All the π products are equivalent to the expression for I_0, divided by $|J_0(v_F)|^2$, where F, a function of m, depends on the particular term in question. The second term applies only to the even diffraction order values and is small, due to the small values of $J_2(v)$. The terms with the infinite sums dominate the asymmetry of the pulse diffraction pattern. They represent a mixing of diffracted light contributions from the individual pulse Fourier components. One sees from Eq. (1-9), in going from m to -m, that the combination of the three terms will add to one side of a diffraction pattern and subtract from the other.

Above equation contains another important piece of information:

Even if pulse amplitudes become high and harmonics are generated, the evaluation of the light diffraction pattern provides a direct measure of the pulse amplitude spectrum.

It is evident from the structure of above equations that higher order approximations can be derived in order to obtain even better agreement between theory and experiment. However, these equations become rather cumbersome in their application and are therefore not included in this Report. They are, however, listed and discussed in [4] and in other references (see list at end of this Report).

Typical Experimental Diffraction Patterns

Below are two sets of figures. They illustrate the growth in asymmetry of actual light patterns as v is increased. The first illustration, Fig. 1-2, shows an approximation to the actual form of a pulsed ultrasonic wave. The figure represents the time history of a single pulse in the wave train and its Fourier amplitude spectrum.

A similar pulsed wave produces the diffraction patterns shown in Fig. 1-3. The actual pulse shape is unique and depends on transducer system characteristics, described in the following sections. It has a pulse modulation frequency, f_o = 2 MHz and pulse repetition frequency, f_p = 125 KHz. Figure 1-3 shows measured diffraction patterns resulting from a pulse peak amplitude corresponding to v = 0.6, 1.5, and 2.5 respectively. The individual diffraction orders are spaced by 125 KHz, as predicted by Eq. (1-5), and their numbers correspond to the component number of the pulse Fourier spectrum. In these patterns the ±16 orders correspond to the 2 MHz component in the amplitude spectra of Fig. 1-2. The next orders, ±17, correspond to the 2.125 MHz component, the ±15 orders to the 1.875 MHz component, etc. Referring to the individual diffraction orders in terms of the frequency value of their corresponding Fourier amplitude component represents a restatement of Eq. (1-5).

The figures show a slight pattern asymmetry that is not significant until the peak amplitude v > 2.0. One might mistakenly conclude that only Eqs. (1-6) and (1-7) are necessary to describe a diffraction pattern in the limit of low acoustic amplitudes. However, the magnitude of the first and second diffraction orders corresponding to the 125 and 250 KHz spectral components are not accurately described by Eq. (1-7). This places a validity limit on the expression to those amplitude components centered about the pulse modulation frequency f_o. For an accurate description of the complete pattern one must use the higher order approximations; e.g., Eq. (1-9) is sufficient to account for all regions of a particular diffraction pattern of interest to studies described in this Report.

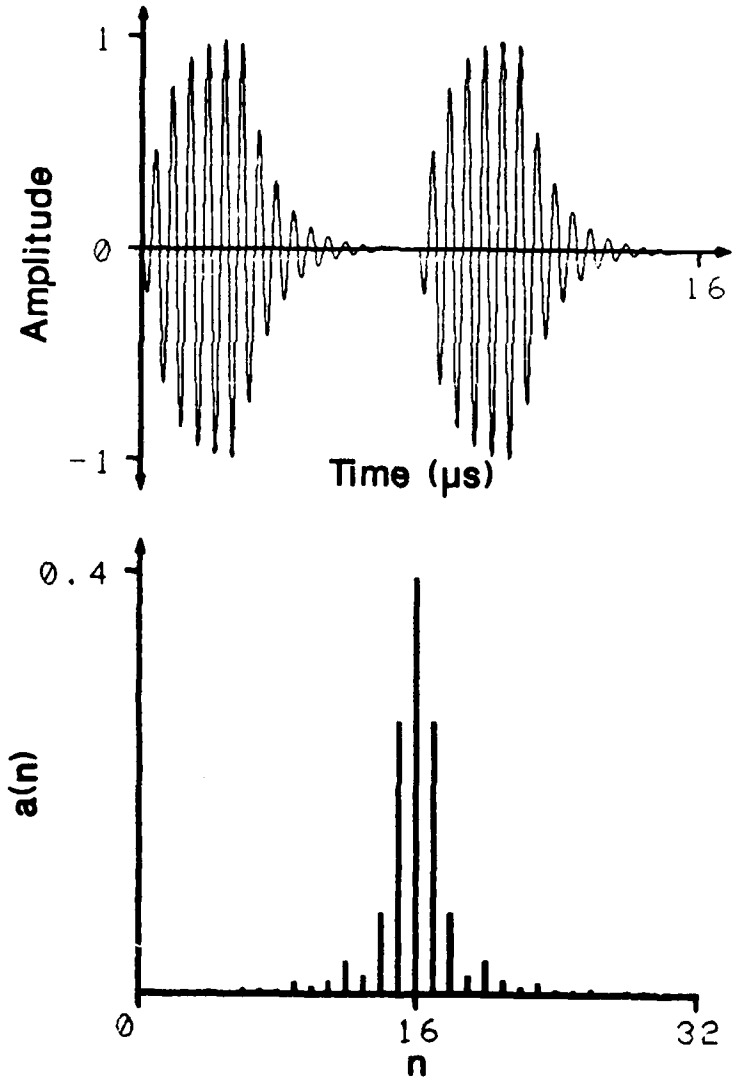

Fig. 1-2. Pulse sequence (top) and its Fourier amplitude spectrum.

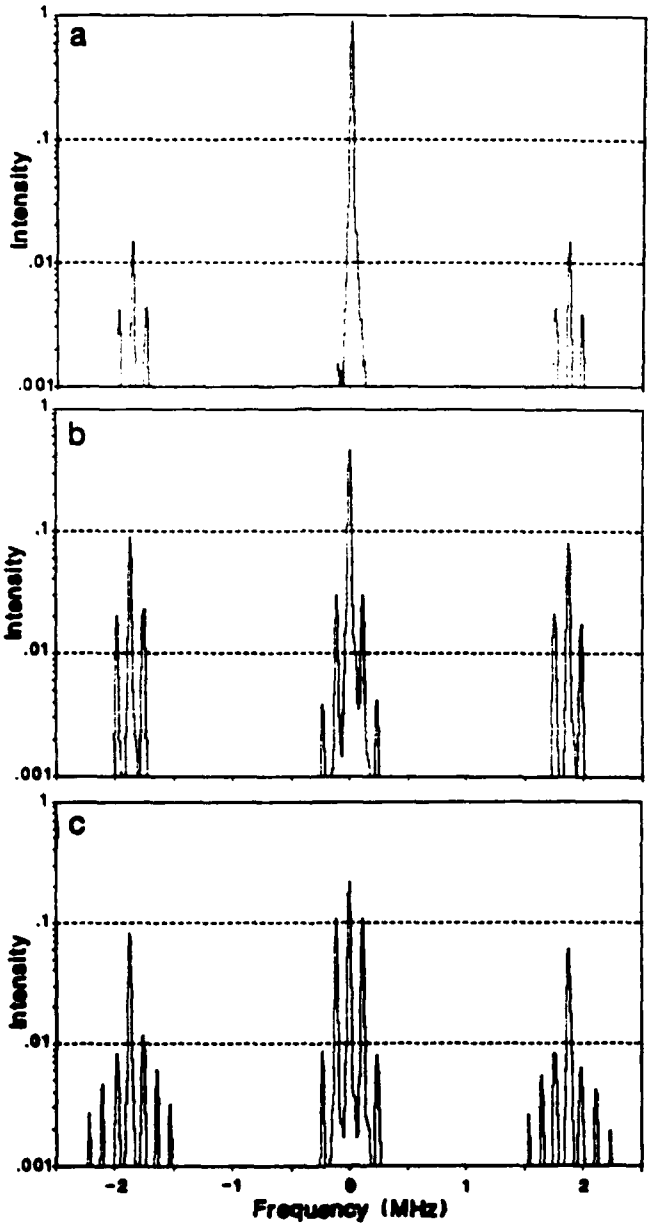

Fig. 1-3. Measured light diffraction pattern produced by a pulsed wave with increasing v-value.

The equations predicting angular spacing of the intensity orders in the Raman-Nath and the present theory are equivalent. In both regimes the smallest spacing corresponds to the wavelength of the lowest frequency component of the Fourier spectrum of the wave under consideration.

This equivalence is demonstrated in Fig. 1-4 which shows the diffraction patterns from ultrasonic waves in transition from pulsed to continuous. The patterns of Fig. 1-4 are due to pulsed ultrasonic waves of a constant duty ratio, 1:1 on to off time. They all have $v_{2MHz} \approx 0.5$ where 2 MHz is the pulse modulation frequency f_o. They are incremented at pulse repetition frequencies 125 and 250 KHz. The last pattern is produced by a continuous, 2 MHz wave. This experimentally illustrates the transition from the pulsed wave theory to the expected Raman-Nath result for continuous waves.

Computational Model

A computational model was developed to calculate the diffraction pattern given the Fourier amplitude and phase spectrum of the input ultrasonic wave. The model is within a complete software package which is used as the theoretical reference throughout.

The pulsed wave described by Fig. 1-2 was used as input to the light diffraction model for comparison to the experimental patterns of Fig. 1-3. The computational output is summarized in the following figure set, Fig. 1-5, where the diffraction peaks are catagorized by order number instead of acoustic frequency.

In comparing the predicted and measured patterns, one sees good agreement between the intensities of all diffraction orders in the first two patterns of the figure sets, that is for $v < 2.0$. As v increases, the low intensity satellites, centered about the existing main orders, show a different structure between the two pattern sets.

The disagreement is due to the input spectrum which is only an approximation to the true spectrum present in the water. The pulsed wave, illustrated in Fig. 1-2, is an estimate of the real

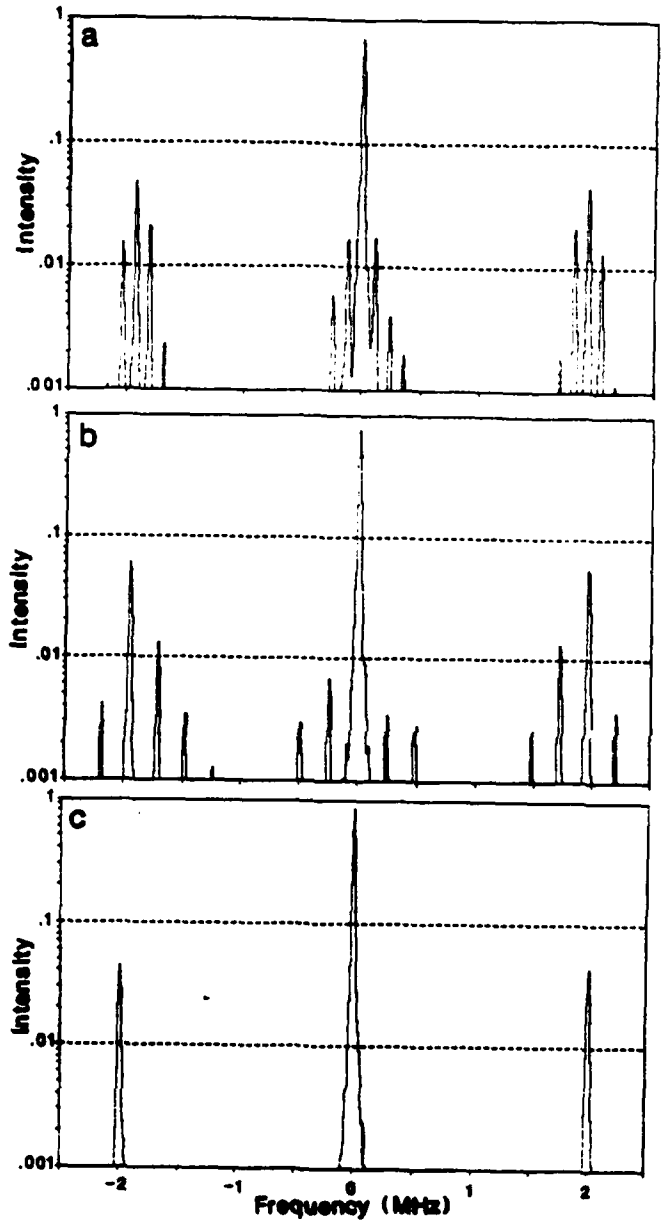

Fig. 1-4. Measured change in diffraction order spacing as function of repetition rate, compared to pattern for continuous wave, (c).

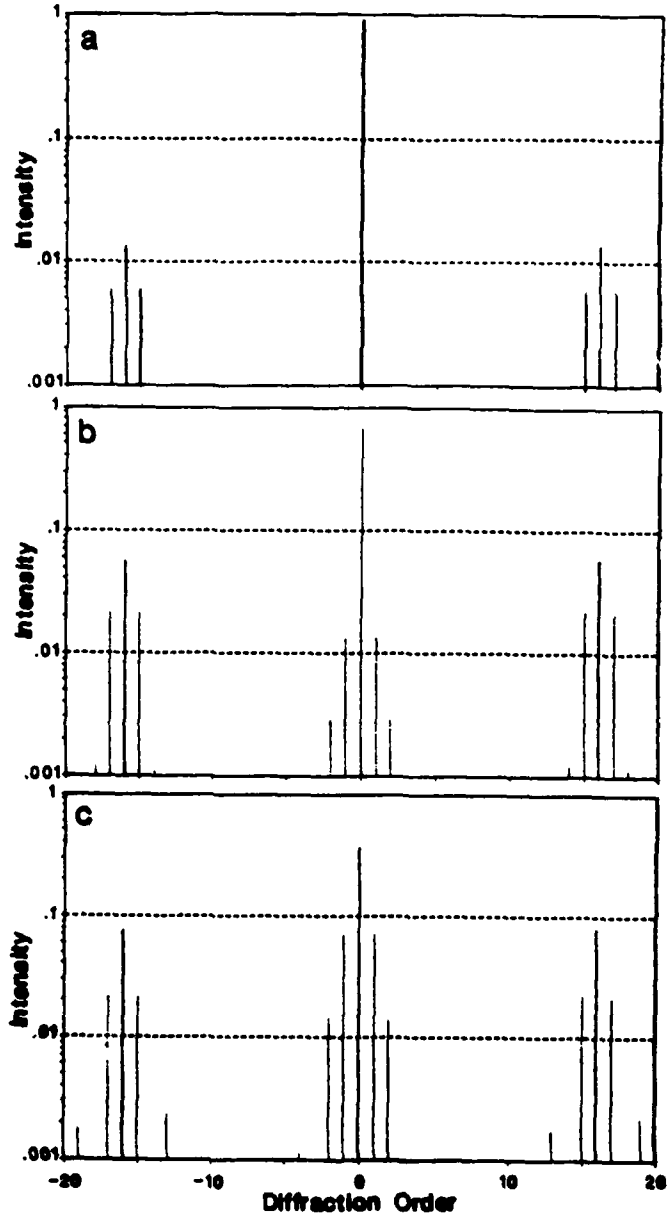

Fig. 1-5. Computed diffraction pattern, based on spectrum given in Fig. 1-2, showing agreement with experimental data given in Fig. 1-3.

form of the wave based on an assumed response time of the transduction system and a knowledge of the pulse duration time. By the technique of Häusler et al. [3] the pulse was modeled from oscilloscope traces of hydrophone probe outputs.

For small values of v, this approximation appears sufficient. If the pulse center frequency is an integral multiple of the repetition frequency then the amplitude spectrum is symmetric about f_o. Such is the case for the example shown in Fig. 1-3 which first appears to be a reasonable approximation to the actual input spectrum. The experimental light patterns shown in Fig. 1-6 are produced by a pulsed ultrasonic beam whose amplitude spectrum is not symmetric about the center frequency, f_o. The pulse parameters for this set are f_p = 97 KHz and f_o = 1.97 MHz. Since the signal was produced by the same transducer system as that of Fig. 1-2, the same rise and decay times of the pulse have been assumed. The first figure is of the measured light pattern. Figure 1-6b illustrates the assumed pulse time history and Fourier amplitude spectrum used as input to the diffraction model. The last figure in the set is of the predicted light pattern for v = 1.0. The intensities, $I_{\pm 1}$ and $I_{\pm 2}$ do not show agreement in the two patterns. According to Eq. (1-9), the intensity of these satellite orders are heavily dependent on the amplitude of the dominant terms in the pulse Fourier spectrum. The two more dominant harmonic terms in the spectrum correspond to the $I_{\pm 20}$ and $I_{\pm 21}$ in the light pattern. Their slight difference, between measured and predicted intensity, is translated throughout the rest of the diffraction pattern.

Clearly, what is lacking is a better understanding of the form of the ultrasonic wave in the medium.

But fortunately, the real form of the ultrasonic pulse transmitted into the medium by a transducer system can be analyzed, using the light diffraction apparatus, resulting in a better definition of the pulsed wave input spectrum.

The use of this analysis results in a much better agreement between the theory oulined above and the various experimental results listed in the following sections of this Report.

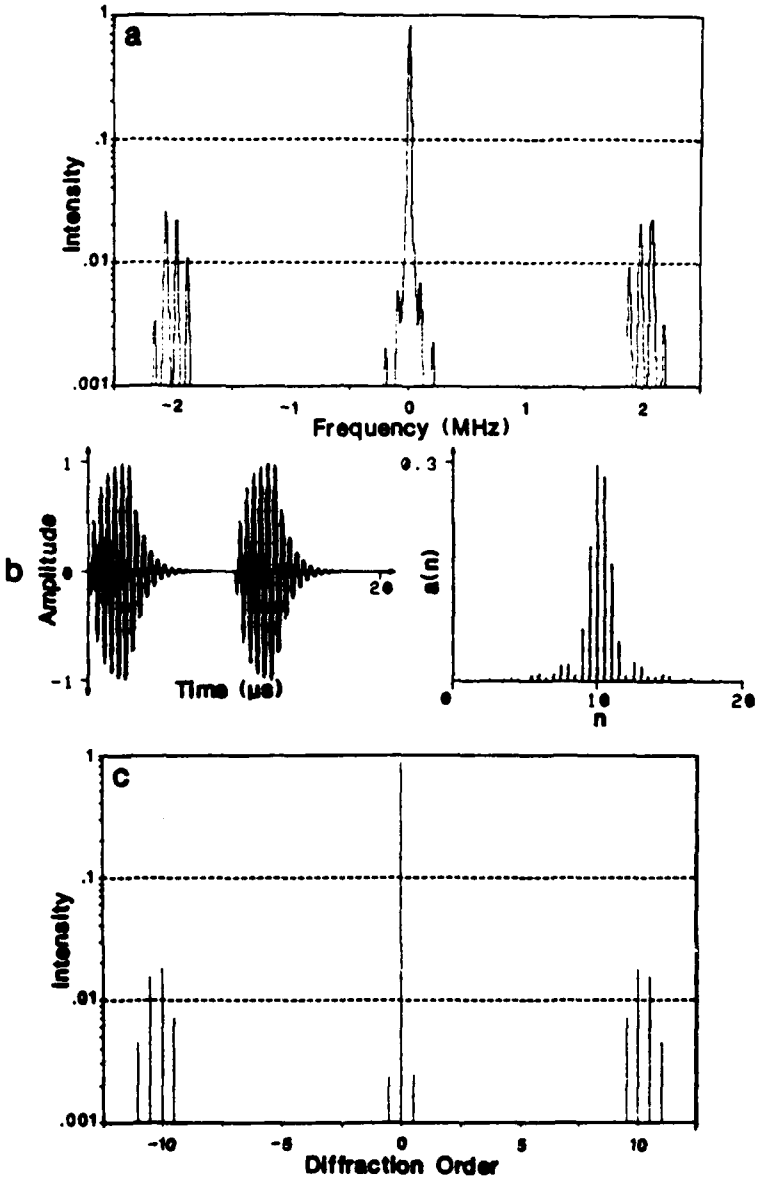

Fig. 1-6. Measured light diffraction pattern (a), produced by a pulse shape (b) whose Fourier spectrum predicts a light diffraction pattern as shown in (c).

REFERENCES

1. L. E. Hargrove, J. Acoust. Soc. Am. **43**, 847 (1968).
2. R. N. Zitter, J. Acoust. Soc. Am. **43**, 864 (1968).
3. E. Häusler, W. G. Mayer, and M. Schwartz, Acoust. Lett. **4**, 180 (1981).
4. T. H. Neighbors and W. G. Mayer, J. Acoust. Soc. Am. **74**, 146 (1983).

Section 2

EXPERIMENTAL SETUP AND PROCEDURE

Fundamental Requirements of the Experiment

A simple Raman-Nath experimental configuration would be sufficient for a study of continuous ultrasonic waves by light diffraction. Standard optical setups of this type set a lower frequency limit for the investigation of continuous ultrasonic waves of about 1 MHz, in water. Given a 1 MHz acoustic wave in water, the Raman-Nath theory predicts a diffraction order spacing which is of the same order of magnitude as the width of a standard He-Ne laser beam. This indicates that the diffraction orders are just resolvable since the order separation increases with frequency.

For light diffraction investigations of pulsed ultrasonic waves, the theoretical constraints on the apparatus are more demanding. The necessary optical resolution is determined through diffraction theory by the pulse repetition frequency. An additional constraint of the theory places a limit on the minimum number of pulses within the illumination window at one time, in order to have sufficient light intensity resolution in the diffraction pattern. This establishes a width criterion for the optical beam. For the present study a minimum pulse repetition frequency of 50 kHz or less is desired. To acquire the same optical resolution as mentioned above for the simple Raman-Nath setup, the apparatus must accommodate a light beam with a sound beam-image plane distance of 25.9 m. The light beam width which defines the interaction region must satisfy 21 » 0.5 cm. This indicates a large optical system is needed for pulsed ultrasonic wave studies.

The following sections describe a light diffraction system with a maximum acoustic spectral resolution of 40 KHz and the ultrasonic beam generation equipment sufficient to test the theories described in the previous section.

Laboratory Equipment - Optics

It has been shown that in order to resolve diffraction patterns from pulsed ultrasonic waves, an optical system requires a long optical path. Early investigations [1-3] used an expanded light beam which focused directly into a photodetector. Thus measurements were taken at the optical image plane.

In this experiment the light beam passing through the ultrasonic wave is collimated and then focused to produce a small diffraction pattern at the image plane. A lens recollimates the light into a set of narrow beams. This second stage of collimation diverges the individual beams, thereby increasing their angular separation. Measurement takes place beyond the image plane where the diffraction orders are further resolved. This effectively increases the separation of orders in a diffraction pattern without requiring a longer optical path.

Figure 2-1 is an overhead schematic of the optical apparatus. The object plane corresponds to the ultrasonic beam in the interaction vessel. To illustrate the possible resolution: if a continuous wave of 1 MHz were to be used, this optical system would produce a diffraction pattern at the screen with an order spacing of 12 cm.

Using mirrors instead of lenses to collimate the light beam reduces the overall size of the apparatus. Individual components of the system are positioned across three relatively large laboratory tables. Random vibrations are reduced by massive mirror mounts and optical benches. The geometrical symmetry of the light path reduces optical phase distortion at the image plane. Phase distortions are further minimized by limiting the size of the light beam reflection angles at the two spherical mirrors, (labeled 12° in Fig. 2-1).

Early diffraction experiments used collimated light beams of circular cross section. In this apparatus cylindrical lenses diverge the light beam in one dimension. Once collimated, the beam has an approximately linear cross section. A comparison of the two cross sections is illustrated in Fig. 2-2. The two cases illustrate the light beam intersecting a nonuniform ultrasonic

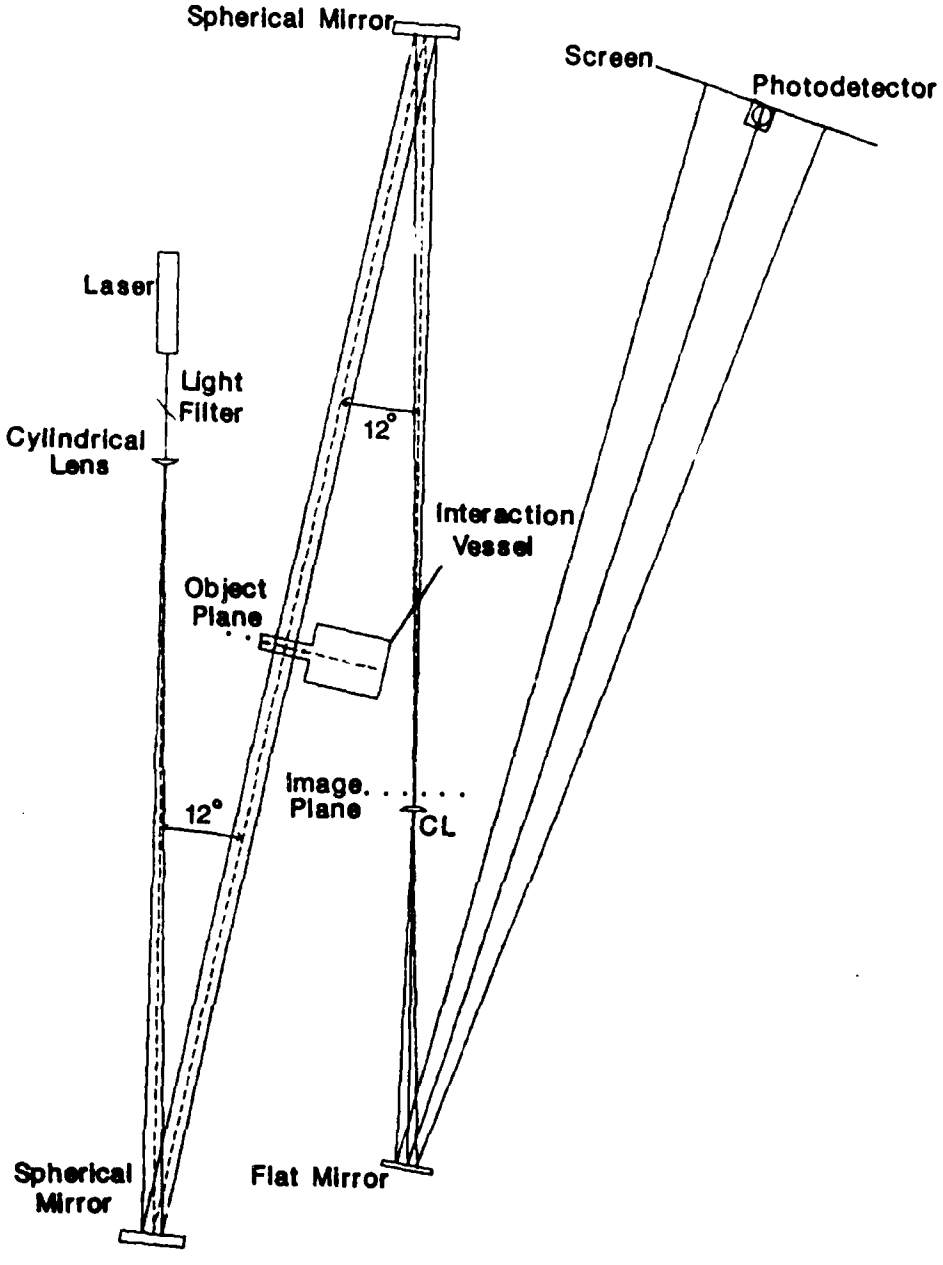

Fig. 2-1. Schematic diagram of the optical arrangement.

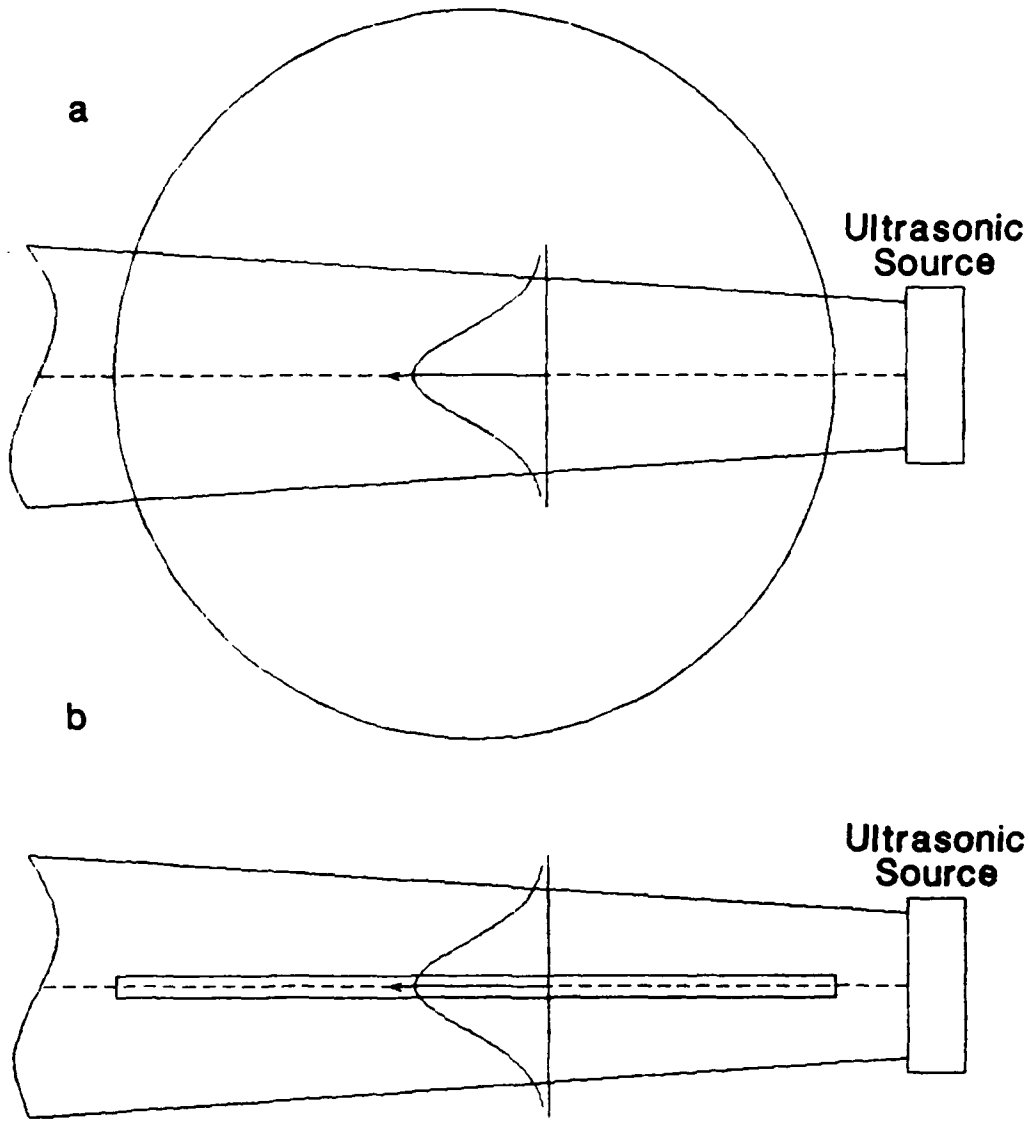

Fig. 2-2. Comparison of collimated light cross section using (a) circular lenses or (b) cylindrical lenses.

beam where the plane of the figure is the object plane.

There are several disadvantages to lens collimation resulting in light beams of circular cross section. Any part of the light beam not participating in the acousto-optic interaction would have to be blocked out, otherwise a diffraction pattern could not be properly normalized. This is illustrated in the first two cases of Fig. 2-3.

The resulting optical apparatus resolves a minimum pulsed ultrasonic wave repetition frequency of 40 kHz. It satisfies the theoretical criteria necessary to study a broad range of ultrasonic wave spectra. The following section describes the transducer system which produces the ultrasonic waves under investigation by the optical apparatus.

Laboratory Equipment - Ultrasonic Beam Generation

The ultrasonic source is contained in a water tank designed to fit in the confined space defined by the optical beam. Its location within the optics was chosen to maximize the object-image plane distance. The tank is made of transparent plastic except for glass windows which allow the light beam to enter normal to the ultrasonic beam. The acousto-optic interaction takes place in a narrow channel of 4.5 cm width bounded by the windows. Acoustic absorbing rubber is placed at the end of the channel positioned such that unabsorbed waves are not reflected parallel to incident waves. The main body of the interaction vessel allows ultrasonic wave propagation distances of up to 45 cm. It holds a large body of water that draws heat out of the interaction channel. The channel is narrow thereby reducing light pattern distortion, due to fluid flow, by minimizing the distance the light traverses in the liquid medium.

The water vessel is large enough to hold a variety of ultrasonic wave source equipment. On top of the interaction vessel, a graduated acoustic bench suspends an ultrasonic source and plate mode goniometer into the main body of the water tank. Both devices are supported by sliding mounts which allow adjustment of source and plate distance from the light interaction region.

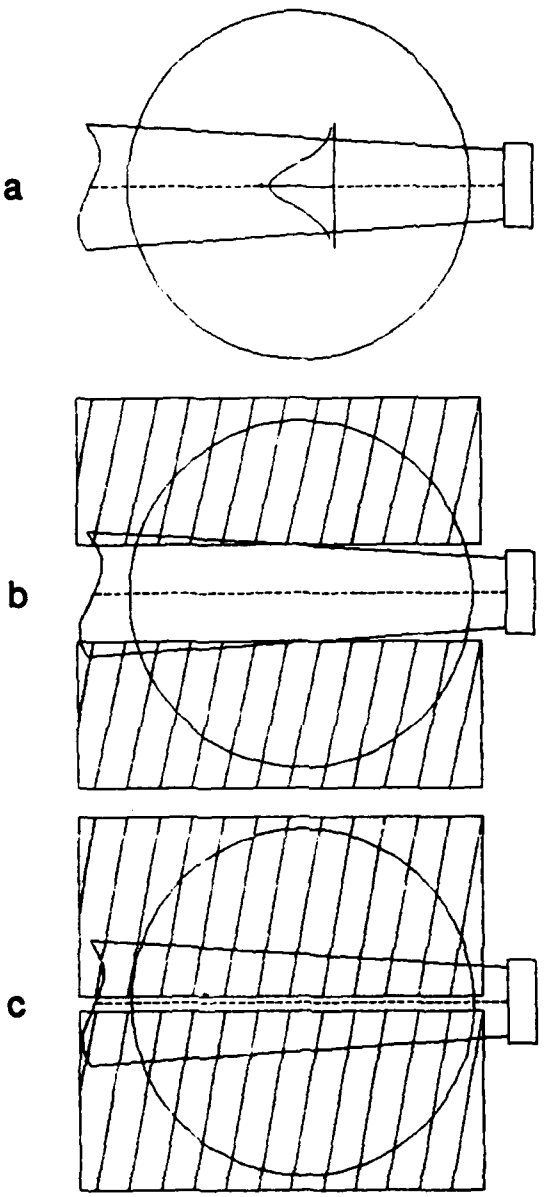

Fig. 2-3. Schematic diagram of requirements for proper light intensity normalization.

The ultrasonic source element is a PZT ceramic disc, 2.5 cm in diameter, which is air-backed mounted in a plastic housing. The mounted element is driven directly from the output of an rf power amplifier which receives an input signal from a computer controlled pulse function generator.

The goniometer produces reflected and transmitted ultrasonic waves incident on solid plates immersed in the water. It rotates a plate sample and the ultrasonic source about a single axis, as indicated in Fig. 2-4. The axis lies along the water/plate interface and is perpendicular to the plane of the incident and reflected ultrasonic beam. Plate and source rotations are controlled from outside the interaction vessel through a linkage of control rods and worm gears. The goniometer positions the plate and source such that the reflected or transmitted wave is directed into the light interaction region.

Proper directivity of the acoustic beam is achieved with a Schlieren imaging system. The light beam of the Schlieren system is passed through the transparent plastic walls of the interaction vessel main body and aligned parallel to the light beam of the diffraction system. The Schlieren system projects an image of the reflected beam onto a screen where an angle vernier ensures proper ultrasonic beam alignment.

Laboratory Eqipment - Light Detection System

A photomultiplier tube is permanently positioned at the image screen. The detector tube is enclosed in a box which holds neutral density filters and a manual shutter with a 3 mm width slit opening. The slit shape and size approximate the zero light beam cross section in the plane of the screen. A dc amplifier converts the tube output current into a voltage proportional to the incident light intensity.

Positioning an individual light beam incident onto the photomultiplier tube, simultaneously measures the relative light intensity and position of each diffraction order. This is accomplished by rotating the flat mirror as shown in Fig. 2-1. The mirror is rotated through a gear box by a stepper motor.

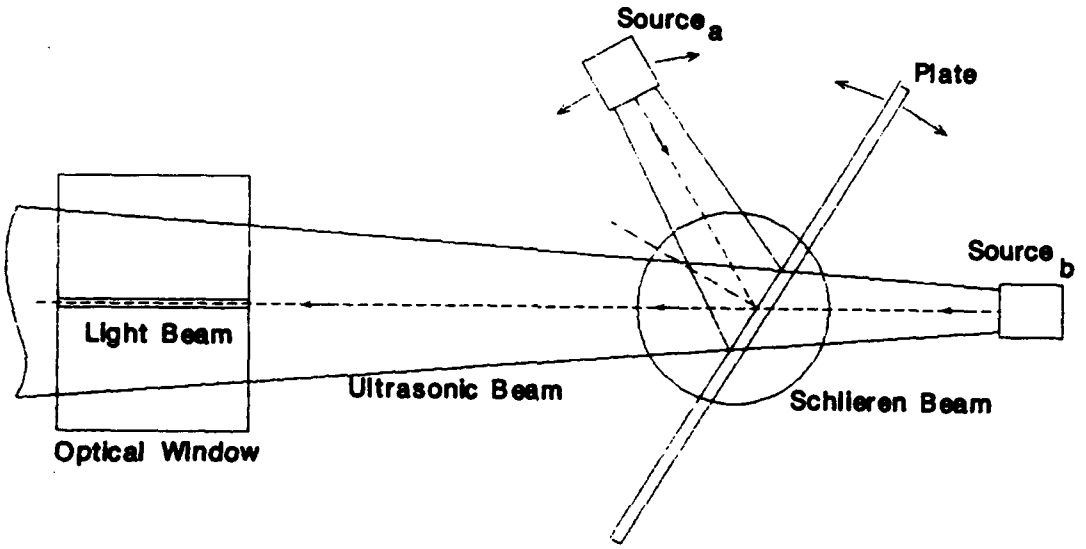

Fig. 2-4. Schematic diagram of goniometer arrangement.

Each diffraction order is then individually passed across the slit opening of the photomultiplier tube box. Thus the diffraction pattern is scanned without moving the photomultiplier tube.

The light intensity range, in a typical diffraction pattern, is greater than a single sensitivity range setting of the photoamplifier. The amplifier has manual, front panel controls which allow it to cover a relative intensity range of over 30 dB However, manual control is impractical when a large volume of data is to be taken. The next section describes the computer automation of the photoamplifier and other laboratory devices.

Computer Automation - Hardware

Due to its relatively long path length, the light beam is subject to fluctuations in position and intensity at the detector. These fluctuations are significantly reduced by the removal of the acoustic signal generating devices and users from the laboratory. Thus, the laboratory has been closed and all experimental adjustments and steps are remotely controlled through a single computer interface cable. The acoustic source is driven through a coaxial cable to the signal amplifier in an adjacent room.

Computer commands, which control individual laboratory functions, are channeled through a TTL driven multi-function board which provides computer read/write ability over 15 individual data channels. Each channel can be switched to either perform digital conversion of an analog voltage with 8 bit resolution, (A/D conversion), or pass TTL logic signals to various control circuits of the data acquisition systems.

The board can perform A/D conversion on all channels simultaneously by a signal from the computer. Data is sent sequentially from each channel over an 8 bit parallel interface to the computer for storage and processing. Most channels are switched into the write mode where they pass computer command signals to other circuit boards.

The intensity range of diffraction patterns in these experiments covers several orders of magnitude, therefore, 8 bit digi-

tal resolution is not sufficient. To overcome this limitation, a separate circuit board was designed to provide computer control of photoamplifier range switching. The switch board receives computer commands through the multi-function board. It consists of a series of TTL controlled dip relays which duplicate the range selector switch of the photoamplifier. Each range setting has 8 bit resolution. If the light intensity seen by the photomultiplier is in the top 10 % of a particular sensitivity range the computer switches the amplifier to a less sensitive range. If the intensity falls into the bottom 10 % the computer switches to a more sensitive range. The 30 dB amplifier range along with 8 bit A/D conversion per channel provides an effective digital resolution of approximately 15 bits.

Diffraction pattern scanning is accomplished through the control of a stepper motor. Electronic pulses from the computer are channeled through the multi-function board to a motor drive circuit, providing control of motor rotation and rotation direction. The motor is connected through a gear box to the flat front surface mirror as shown in Fig. 2-1. The motor-to-mirror gear ratio is such that a single motor step produces an effective mirror rotation of 2.5×10^{-5} radians. This corresponds to a diffraction pattern translation of 0.15 mm/step. Due to the long optical path the number of motor steps between diffraction orders is proportional to the actual order spacing. The computer simply has to keep track of motor steps to assign relative position to an intensity measurement.

The pulse function generator produces the electronic signals sent to the ultrasonic source. A separate IEEE-488 interface controls the pulse function generator. Therefore the computer fully manages experimental input, procedure and output.

Computer Automation - Software

Various software program modules were developed for a personal computer to manage specific laboratory functions. The modules were written in the Pascal programming language but can be written in other appropriate computer languages.

Control of the pulse function generator is accomplished through individual program procedures for the IEEE-488 standard interface. A single program module builds command strings from parameters input by the user. The interface converts these commands into a bit pattern read by the function generator.

Individual procedures were written to control motor direction and step by a poke to the appropriate channel on the multi-function board. It also removes gear backlash after each change of motor direction.

Intensity measurements, from the photoamplifier, enter the computer through the multi-function board. A procedure pokes the read channel monitoring the photoamplifier output and stores the resulting 8 bit number in an internal buffer. If the resulting value represents an intensity in the middle of the present photo-amplifier sensitivity range the procedure passes the value for storage. The motor control procedure then tells the motor to rotate a step, then read, then step, etc.

Initial measurements of light patterns revealed that the relationship between photomultiplier output voltage and incident light intensity was not linear. A simple routine was followed in which calibrated neutral density filters were placed into the incident light. Intensity measurements provided a comparison of the amplifier response against calibrated light intensity response for each sensitivity range. The response was modeled, inverted and incorporated into a linearization procedure which is called by the read procedure. Thus photoamplifier response is made linear within the controlling software.

These program modules work together and provide great flexibility in this study of light diffraction by ultrasonic waves. The following sections describe the integration of individual control modules into one main program which performs the entire experimental procedure.

Experimental Procedure and Data Processing - Digitizing a Light Diffraction Pattern

Individual Pascal modules that control laboratory functions

are integrated together into a single control program which performs complete experiments.

After final apparatus adjustments are made the experiment is performed. Experimental parameters are loaded into the program and divided among two information arrays called the hard and soft stacks. In general, the hard stack contains input data that the computer neither has control over nor is able to measure, therefore remaining constant over a series of runs. Such information includes: the user choice of either frequency or amplitude variation mode, ultrasonic wave propagation distance, acoustic beam configuration, characteristic frequency of ultrasonic source element, number of passes and runs to be performed, specific function generator output voltage needed to minimize I_o.

The soft data stack contains acoustic signal input variables to the pulse function generator. These include: pulsed or continuous wave mode, peak voltage amplitude, center frequency, repetition frequency, and pulse width. These parameters make up the command string sent to the pulse function generator through the IEEE-488 interface. The program saves diffraction data in a disk file. The filename is derived from a concatenation of the soft stack variables.

Once all hard and soft stack variables are entered, the program begins its run. With the ultrasound disabled the program translates the zero order to a position left of the detector. It changes direction, removes motor backlash, and steps the zero order to the right across the light detector slit. Between each translation step the program reads the light intensity, makes a linear adjustment of the resulting 8 bit value, multiplies according to the photoamplifier sensitivity range setting and stores the result along with motor step number in an array. This continues until the zero order is an equal distance to the right of the detector slit.

This initial procedure maps the form function of the zero order. The form corresponds to the $(\sin x/x)^2$ function. The actual measured form is similar to a $(\sin x/x)^2$ function but also displays a Gaussian character, which is in agreement with the

result of Hargrove[7]. Since this experiment assumes fully resolved diffraction patterns, an individual diffraction order intensity is acquired without performing a deconvolution of the total pattern and the form function. Therefore the diffraction pattern normalization constant equals the peak light intensity value of the form function. Since diffraction order position is measured relative to the zero order, the peak form intensity is assigned a step number position of 0. The form function data are saved along with each diffraction pattern data set.

The program changes motor direction and the pattern is now moved to the left until the rightmost diffraction order to be measured passes beyond the detector slit. The same intensity measurement procedure is followed as that which read the form function.

For each pass of the pattern the program normalizes the data array to the peak intensity value of the form function. This procedure results in a digitized diffraction pattern. The process takes a finite amount of time which depends on the shape of the individual diffraction pattern. For example, one pass of a simple Raman-Nath pattern and its form function can take from 2 to 7 minutes. Individual diffraction order intensities significantly fluctuate over such time periods. This is a result of spurious laboratory vibrations, laser moding, temperature gradients, light detector instability, atmospheric and fluid currents, etc. These inherent system fluctuations can alter the reproducibility of results. The following section describes the steps taken to arrive at more accurate values of diffraction pattern measurements.

Experimental Procedure and Data Processing - Multiple Passes and Runs

Most system fluctuations are random in nature and make necessary the acquisition of data from more than one pass of a pattern. This is easily done within the computer program. The data storage array is given another dimension allowing each pass to be saved in parallel to the previous pass. An individual

intensity measurement is ignored if it does not appear in previous passes. Readings are deleted from previous passes if they do not appear in the latest pass. Therefore each individual array, corresponding to a single pass, ends up with the same number of readings allowing them to be averaged. For fully resolved patterns, deleting nonrecurring measurements clips the low intensity readings at the edge of an order's form function but leaves the peak intensity values intact.

An individual program run can average up to ten passes of the pattern, however, averaging three to five passes attains sufficient reproducibility of experimental results. Diffraction pattern measurements, from identical pulsed ultrasonic wave configurations, show no significant change over time.

Experimental Procedures and Data Processing - Miscellaneous Program Features

According to the diffraction theory, a light diffraction order corresponds to an acoustic spectral order. The experiment expresses an order number in terms of the acoustic frequency component it represents, i.e., a simple transformation provides

C (motor step number) = frequency of order.

The constant C is approximated from measurements of continuous wave diffraction patterns. The program makes this variable transformation prior to storing acquired diffraction pattern data. Thus position of light intensity measurements are expressed in frequency rather than motor step or order number.

The program enhances fully resolved diffraction orders by artificially including zero intensity readings at the edge of an order's form function. This is done for graphing purposes and helps to separate the orders for later analysis.

All data contained in the hard and soft stacks are included in the output data file for reference. The elapsed time of data acquisition, time of day and date of the experiment are stored along with the diffraction data. A printout of a typical output

data file is shown in Table 1, presented at the end of this Section.

A coordinated series of program runs is discussed below, where the measurements are of Raman-Nath type diffraction patterns produced by continuous ultrasonic beams. This run series reveals characteristic information about the ultrasonic source. These source characteristics are used in studies of pulsed ultrasonic waves.

Measuring Spectral Bandpass of an Ultrasonic Source - Electromechanical Approach

Behavior of a specific transducer system resulting from an induced stimulus is difficult to model exactly. Various experimental techniques are used to better model transducer response characteristics. Acquiring the response typically involves applying a known stimulus to the transducer and measuring the resulting output. A comparison of the known input and measured output reveals valuable response information about the transducer system.

Acoustic source response is usually measured by electronic techniques. An experimental procedure typically starts by sending into the system a single electronic pulse of known spectral composition. Usually the shape of the pulse is sufficiently narrow such that it takes on a delta function character. The Fourier amplitude spectra of a delta function is constant for all frequencies. Physically, the transducer sees all frequencies of equal amplitude. In converting electrical energy into mechanical oscillation a transducer will pass only those frequencies allowed by its response. The resulting acoustic output signal contains the band of frequencies passed by the transducer system. The signal propagates a finite distance in the medium and is measured by a previously characterized transducer receiver. Acoustic energy is converted back into an electronic signal. Analysis is performed where a deconvolution removes the known receiver frequency response. The resulting continuous spectra represents the frequency bandpass of the acoustic source.

With modern electronic digitizing equipment this transducer characterization procedure is routine. However the measurement is only as accurate as the previous characterization of the receiver. Also, most receivers can only measure a part of the acoustic beam at one time. A direct noninvasive measurement of the acoustic signal, at its source, in the medium is needed. This would provide a more accurate characterization of the transducer system.

Interaction with a light beam produces no measurable distortion of an ultrasonic wave. The light probes noninvasively. The following section describes an experimental procedure to directly measure the frequency response of an ultrasonic source by light diffraction.

Measuring Spectral Bandpass of an Ultrasonic Source - Light Diffraction Approach

Measuring the harmonic response of an ultrasonic source with light diffraction is, in theory, the same as the electromechanical approach. Frequencies of equal amplitude are sent into the transducer and the resulting output is measured. However, introducing a single delta function pulse into the source would not produce a measurable diffraction pattern. This is implied by the optical beam width constraint equation of the diffraction theory. Another method is used which sends a specific range of frequencies, each equal in amplitude, to the ultrasonic source, however, they are sent individually at different times.

Each frequency is input continuously thus producing a simple Raman-Nath type diffraction pattern. The data acquisition system digitizes each pattern and saves the data set. It increase the pulse generator output frequency a small increment keeping the input voltage constant. This frequency stepping continues until the desired response range of the ultrasonic source is measured. For this apparatus, the full resonant range of the transducer source element is measured in two overnight program runs.

The resulting series of light patterns are sifted to extract the peak intensity values of the individual diffraction orders.

Since they are simple patterns, each holds only the $I_{\pm 1}$ and I_o, Raman-Nath diffraction orders. The normalized intensity values are converted by a computer program into values of the Raman-Nath parameter, v. Values of v, with standard deviations greater than 25 %, are ignored. This involves only I_o diffraction order readings at very low values of v. This is due to the functional form of the I_o to v conversion and the relative range of light intensities in the patterns. A curve is derived by an average of no less than 2 values of v to each value of frequency. The resulting normalized response curve for a 1 MHz ultrasonic source is shown in Fig. 2-5.

In actuality, this curve characterizes more than the response of the PZT ceramic element. It represents the transfer function of the entire transducer system, including the rf power amplifier, coaxial cable and mounting of the PZT element.

The light integrates across the entire width of the acoustic beam. The light beam effectively measures the entire acoustic beam at the output element of the system. Since the light beam interaction is noninvasive, there is no light beam transfer response and no deconvolution to perform.

The results of the ultrasonic source response measurement are used for the evaluations of all experimental inestigations involving pulsed wave spectra. The modelled pulse is used as an input to the propagation model, the output of which is input into the diffraction model. The resulting theoretical diffraction patterns are compared to those measured by the experimental apparatus.

Measuring Spectral Bandpass of an Ultrasonic Source - Modeling an Input Pulse Spectrum

This section reports on a technique, using the acquired transducer characterization curve, to model the pulsed wave spectra produced by the ultrasonic source. The pulsed signal generator, providing input to the transducer system, produces an electronic pulse of ideal shape. This pulse shape is easily modeled from soft data input parameters, from which a Fourier spectrum is constructed.

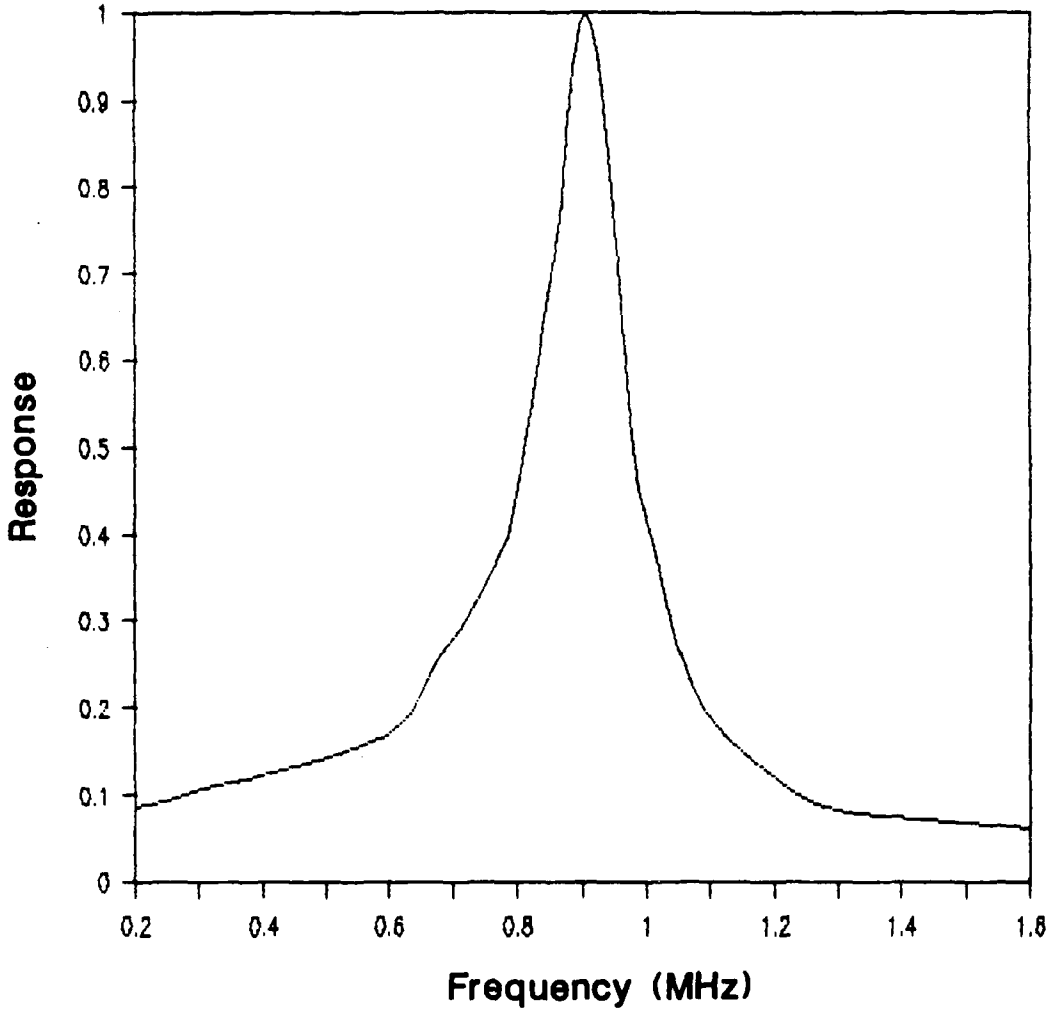

Fig. 2-5. Normalized response curve for a nominal 1 MHz transducer.

However, the generator signal is sent through the transducer system which produces the ultrasonic pulse in the water medium. A convolution of the measured transducer response and the generator output spectra provides an accurate approximation to the actual pulsed wave spectrum in the water medium. The following illustration (Fig. 2-6), shows the pulse modeling technique. It shows a typical pulsed wave output from the pulse function generator. This general shape is the same for all pulsed waves, output from the generator, regardless of the values of f_p, f_o and burst #, (number of single wavelengths in the pulse). The particular input data used to generate the first figure is:

f_p = 66.0 kHz
f_o = 988.0 kHz
burst # = 5.

A Fourier analysis of this pulse provides the first graph of the amplitude spectrum in Fig. 2-6 which is used in a discrete convolution with the transducer system response of Fig. 2-5. The resulting spectrum and reconstructed pulse time history is shown in the second graph.

The resulting spectrum is used in the diffraction model to predict the shape of the diffraction pattern produced by the wave in the medium. An experimental pattern is acquired by positioning the ultrasonic source at the edge of the light beam. Figure 2-7 compares the diffraction model prediction to the measured pattern. Good agreement is seen in most regions of the pattern. Slight deviations are attributed to measurement error in the response curve at frequencies off the value of the center frequency.

The diffraction theory equations indicate the higher intensities of the center frequency diffraction orders are what give rise to the intensities of the higher diffraction orders. Therefore, a small percentage error in the first set of satellite orders would produce more profound percentage error in the second set of satellite orders. With this in mind, the small deviations

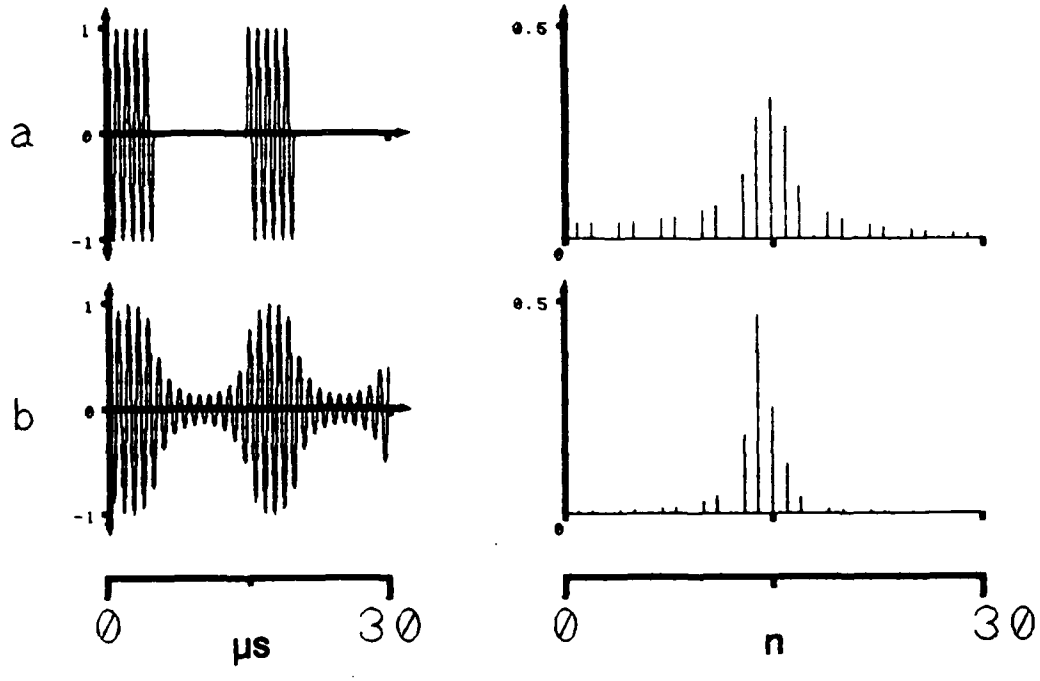

Fig. 2-6. (a) Electronic source signal and its Fourier spectrum; (b) calculated transducer response and its Fourier spectrum.

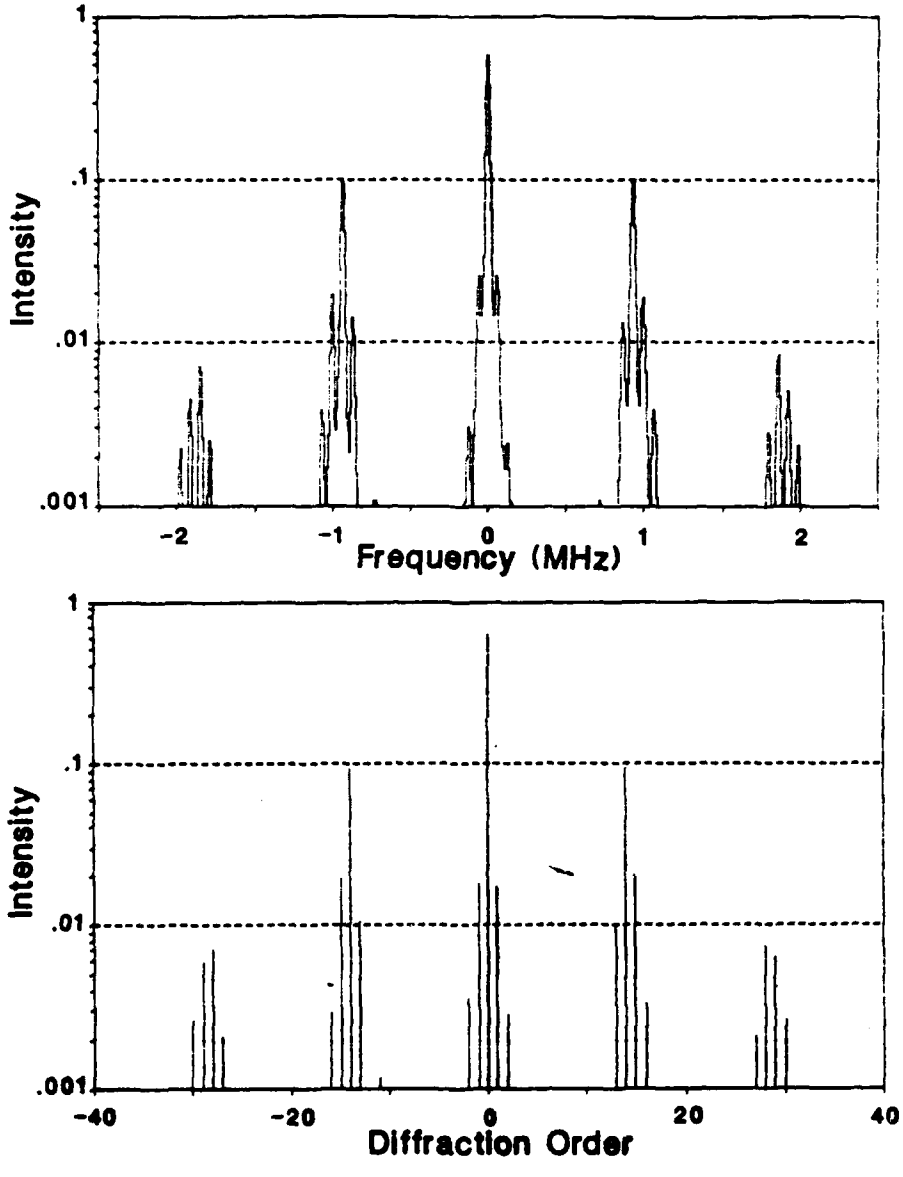

Fig. 2-7. Calculated diffraction pattern (bottom figure), based on results shown in Fig. 2-6, and corresponding measured light diffraction pattern (top figure).

in the second set of satellite diffraction orders, which are evident in the experimental results shown, indicate the pulse amplitude spectrum model is basically accurate, otherwise the disagreement between theoretical prediction and experimental results would be much larger.

Table 1.

Filename is C:\DATA\PULSE\STRAIGHT\S54-86.521,
CW estimate of v = 1.50, Prop. dist. = 4.5 cm.
Taken February, 15 at 6:44 hours.
198 = number of reads in pattern.
Run elapsed time = 0:39:57.46.
Lab Temp. = 20.5°C. Tank Temp. = 20.3°C.
Intens. Norm. = 22960.0000 ± 176.9565
Rep.Rate = 8.00 µs, # of waves = 6,
Frq = 2.00 MHz, PreAmp. = 54.9 mV.

#	Frq.Mhz	Intens.	Std.Dev.
.	.	.	.
8	-3.8346	0.000000	0.000000
9	-3.8257	0.000583	0.000339
10	-3.8168	0.001181	0.000499
11	-3.8078	0.001860	0.000360
12	-3.7989	0.001613	0.000595
13	-3.7899	0.000748	0.000270
14	-3.7810	0.000000	0.000000
.	.	.	.
93	-0.0268	0.031743	0.003527
94	-0.0179	0.132067	0.022186
95	-0.0089	0.484767	0.082469
96	0.0000	0.726837	0.034543
97	0.0089	0.492153	0.034121
98	0.0179	0.150547	0.048896
99	0.0268	0.020473	0.008328
.	.	.	.
147	1.9844	0.006192	0.001448
148	1.9933	0.020155	0.004206
149	2.0022	0.040323	0.004243
150	2.0112	0.040982	0.001873
151	2.0201	0.022482	0.004242
152	2.0291	0.005645	0.002218
153	2.0380	0.002026	0.000721
.	.	.	.

25 = number of reads in form function.

#	Frq.Mhz	Intens.	Std.Dev.
.	.	.	.
10	-0.0268	0.192298	0.030040
11	-0.0179	0.362663	0.053232
12	-0.0089	0.667455	0.111581
13	0.0000	1.000000	0.007707
14	0.0089	0.708689	0.119207
15	0.0179	0.164826	0.086132
16	0.0268	0.025269	0.003851
.	.	.	.

REFERENCES

1. K. L. Zankel and E. A. Hiedemann, J. Acoust. Soc. Am. 31, 44 (1959).
2. L. E. Hargrove, K. L. Zankel, and E. A. Hiedemann, J. Acoust. Soc. Am. 31, 1366 (1959).
3. M. A. Breazeale and E. A. Hiedemann, J. Acoust. Soc. Am. 30, 751 (1958).

Section 3

PROPAGATION AND REFLECTION

The initial considerations of wave propagation and reflection presented around the turn of the century by Lord Rayleigh and seismologist like Knott all consider plane infinite waves. This simplifying approach is acceptable in many cases, except when the wave under consideration is a relatively narrow ultrasonic beam of continuous waves or when the ultrasonic signal consists of a series of pulses containing a few wave trains in the low-MHz frequency range.

In these cases quite a number of new parameters must be considered in the calculation of propagation and reflection characteristics. Much of this background work was performed in this Laboratory in the past; therefore, only the most important features will be mentioned below as background information for the new results concerning propagation and reflection of multifrequency waves (bounded, high amplitude, or pulsed ultrasonic waves) described in more details in the present section.

Propagation and Reflection of Bounded Beams:

A bounded ultrasonic beam propagating through a fluid to an interface and being reflected back into the fluid is a problem of wide interest. As just mentioned, many aspects of the problem have been explored [1-4]. A model which extends existing work in the fields of propagation, reflection, harmonic generation, including spectral filtering, and integrates the results into a cohesive and comprehensive system, was lacking.

The ultrasonic system under consideration consists of an initial beam propagating through a medium, reflecting from a liquid/solid interface, and continuing to propagate after reflection and possibly transmission when the reflector is a solid plate. The three major physical mechanisms affecting propagation are geometrical spreading, attenuation and harmonic generation.

Harmonic generation arises due to the nonlinearity of the medium, which transfers energy from the fundamental to higher harmonics and from one harmonic to another. On the other hand, attenuation of a propagating beam is caused by the absorptivity of the medium while spatial spreading is due to the finite aperture of the beam. Should these mechanisms act independently from each other, the propagation problem for a bounded beam would be much less complicated. The fact that these mechanisms indeed compete with each other in affecting the propagation characteristics is the principal reason why a satisfactory solution has not been obtained for the complete propagation equation, i.e. the generalized Burger's equation.

In the plane wave regime, approximate analytical solutions have been established for the three special cases, where one of the three mechanisms are assumed to be dominant [5]. Recently, Haran and Cook [6] treated the two mechanisms of attenuation and harmonic generation with equal footing, neglecting the spreading term. They were able to derive an iterative algorithm to solve this form of the Burger's equation numerically for plane-wave propagation. A similar algorithm, although expressed in a slightly different form, had also been developed by Trivett and Van Buren [7] to treat propagation of plane, cylindrical, and spherical waves. This result is rather significant in that it provides a complete solution to plane-wave propagation in a non-dispersive medium. Recent work in this laboratory lead to an extension of this solution to treat propagation of ultrasonic bounded beams.

Reflection of an ultrasonic beam from a liquid-solid interface has been investigated by a number of researchers [8-11], using various numerical and analytical approaches. The analytical approaches are usually constrained by certain approximations, such as incident Gaussian profile, incidence near the Rayleigh critical angle, and field intensity given at the interface only. To compute the reflected profile for an incident beam having an arbitrary profile and impinging at the reflector at any angle of incidence, the numerical algorithm developed by Ngoc and Mayer [9] was employed. Since an ultrasonic beam, which has propagated

through a nonlinear medium, contains various harmonic components in addition to the fundamental, the Ngoc and Mayer's algorithm will have to be extended to treat a multi-frequency incident beam.

Propagation and Reflection of Bounded Beams - Sample Results

The capabilities of the computational model [12] can be best illustrated through a complete sample run. The model was applied to an incident Gaussian beam propagating through water and being reflected from a stainless steel plate. The initial beam was taken to be of a single frequency, 2.98 MHz, with the peak intensity being 1W/cm . Standard values of the sound velocities, attenuation coefficients and densities were used for water and stainless steel, while the nonlinear coefficient was chosen to be B/A = 5.5.

The first propagation program was started with the following programming parameters: beam width = 2.0 cm, propagation distance = 20.0 cm, and incremental step of propagation = 0.05 cm.

The computational results which describe the intensity profiles at selected propagation distances are presented in Fig. 3-1. This figure essentially shows the process of harmonic generation as the beam travels from the starting point to about 15.0 cm away. Within this relatively short distance, one can recognize a significant presence of the first five harmonics. The fundamental component does not attenuate appreciably, but the harmonic content does grow significantly as shown on the 0-50 dB scale.

The program for the reflection coefficient was activated and two passes through this program were made to select the incident angle of interest. The first pass examines the coefficient for incident angles of 0 to 60 degrees, and the second focuses on the much narrower range from 30 to 34 degrees to better establish a plate mode for special consideration, which is about 32 degrees in this case.

For the fundamental component, the incident angle was chosen to correspond with a plate mode of resonance; the reflected

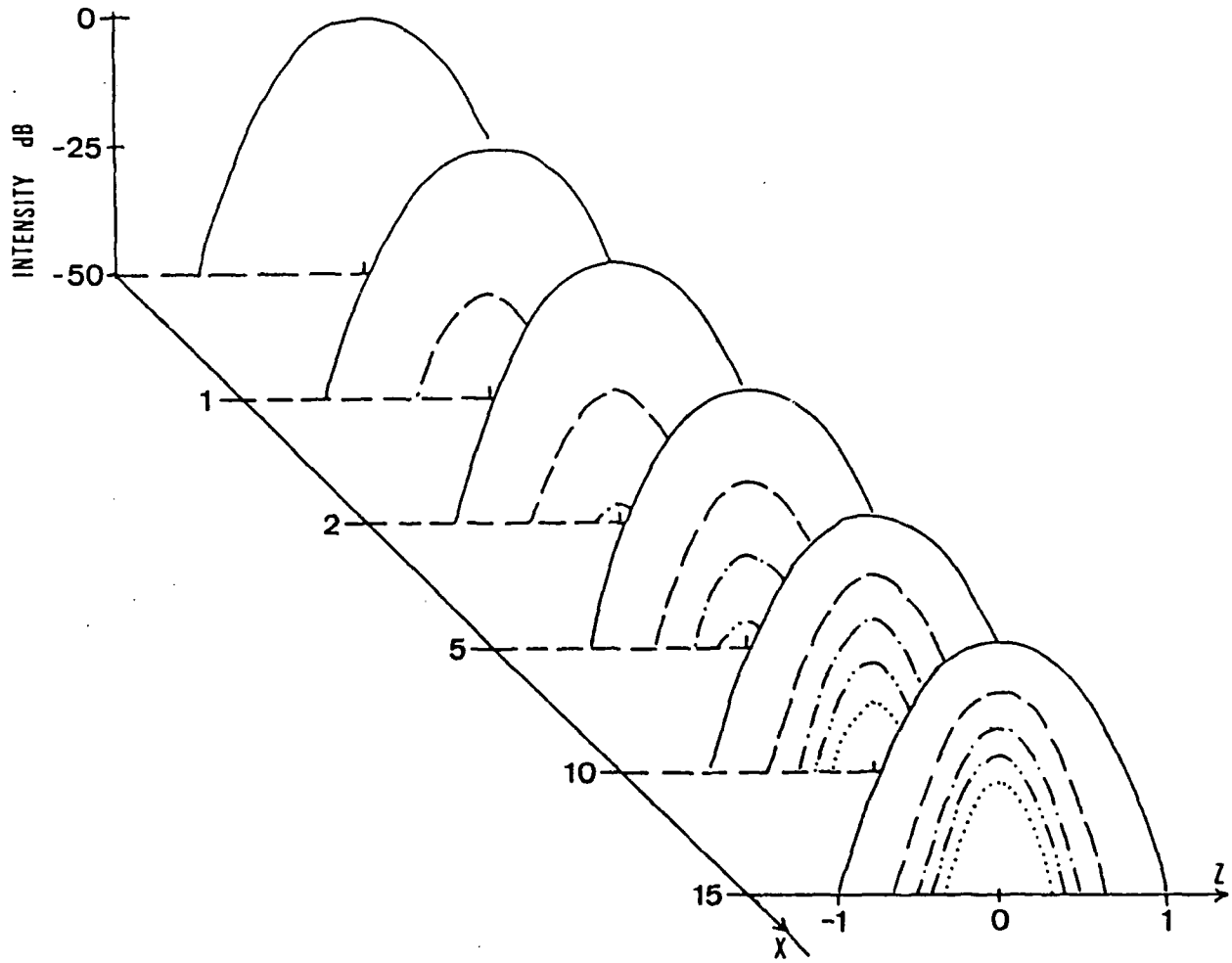

Fig. 3-1. Intensity profile calculated for fundamental frequency and increasing number of higher harmonics.

profile, therefore, displays the distinct nonspecular features of beam split, beam displacement, and trailing field. For the second harmonic, there exists a slight displacement in the reflected profile, but the other nonspecular effects practically disappear. For the third harmonic, the associated range of incident angles does not include any plate mode, and the reflected profile is thus essentially specular.

Figure 3-2 presents the intensity profiles of the first five frequency components, as the beam travels away from the reflecting interface. Within the first few centimeters of propagation, there are not many discernable changes in the profiles, except for the higher harmonics, where attenuation has taken a quicker effect in reducing the intensity level noticeably.

The techniques and some of the results which were used to solve the problem of the multi-frequency bounded beam [12] were also considered in the treatment of the problem of pulse propagation and reflection as investigated by acousto-optic techniques.

Pulse Propagation and Reflection - Basic Parameters:

This subsection deals with the essential features of finite amplitude wave propagation and the reflection and transmission of finite amplitude pulses from flat plates. Since the focus of this Report is on the use of the acousto-optic technique as a noninvasive measurement tool to investigate acoustic pulse interactions, only the pertinent features of the theories are summarized.

Initially, in the study of acoustic waves in continuous media, the theory assumes that the disturbance amplitude is small, that is, the parameters of the medium disturbance, pressure and density, only slightly deviate from their equilibrium values, p_o and d_o. As a consequence, the solution of the wave equation describes a harmonic disturbance that maintains its shape during propagation. Therefore, for small acoustic amplitudes one assumes a linear behavior and omits the nonlinear terms in the equations of motion. The result for a traveling plane

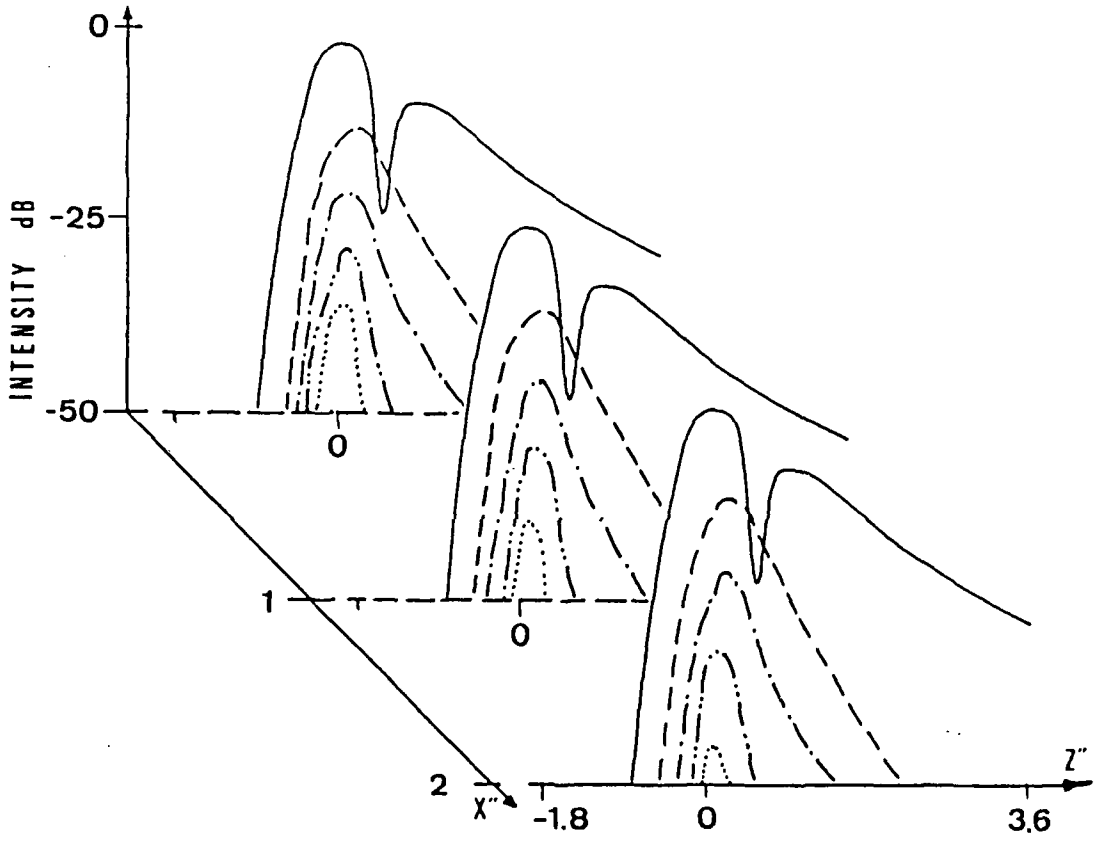

Fig. 3-2. Calculated intensity profiles for fundamental frequency and higher harmonics, after critical angle reflection.

wave solution is the following relationship between the wave vector and the frequency

$$k_o = w_o/c_o(1 - i\alpha' w_o). \tag{3-1}$$

The quantities k_o, w_o, and c_o refer to the wave vector, frequency, and wave velocity. It is assumed that attenuation, α', is due to the viscous and heat conductive properties of the medium.

The resulting solution to the wave equation,

$$u = u_o\, e^{-\alpha' wo^2 x}\, e[iwo(t - x/co)], \tag{3-2}$$

describes a monochromatic wave whose initial particle velocity amplitude, u_o, decreases exponentially with distance, x, from the source and has a quadratic frequency dependence.

One should know whether one has an acceptable approximation if the nonlinear terms in the wave equation are suppressed. Two parameters, frequently encountered in nonlinear acoustics, are the Mach number, M, and the acoustic Reynolds number, Re, which are defined by

$$M \equiv u/c_o, \tag{3-3a}$$

$$Re \equiv u_o/(2c_o^2\alpha' w_o). \tag{3-3b}$$

These values are derived from a comparison of the nonlinear and linear terms within the wave equation, the solution of which is Eq. (3-3). The linear wave theory is considered appropriate if M, Re « 1. The first restriction is satisfied for most problems of acoustics. However, even for moderate acoustic amplitudes, Re is of order unity. In this case, not only dissipation, but the effects of nonlinearity must be considered.

Propagation and Reflection - Interplay of Nonlinearity and Attenuation:

Experimentally, as they propagate in nonideal media, finite amplitude waves exhibit significant changes in shape which are

not simply due to attenuation. In the nonlinear theory, the higher order derivatives and powers of p', d' and u can no longer be neglected in the governing equations.

The first development is that of the exact Riemann solution, for an ideal medium, which predicts that individual disturbance points within the wave profile move at the speed

$$U = c_o + \varepsilon u \tag{3-4}$$

where ε is a medium constant. This indicates that this velocity distortion tends to shape the wave profile into a sawtooth. The steepening continues until, at $x = x_d$, a discontinuity develops in the wave profile indicating, in theory, a shock front character. This specific travel distance is given by

$$x_d = c_o/w_o \varepsilon M, \tag{3-5}$$

where M is the Mach number. The deformation, from a sinusoid to sawtooth wave, represents a transfer of energy from lower to higher harmonic terms in the Fourier spectrum of the initial wave profile.

The theory is applicable to both fluids and gases with exception that ε, the medium constant, be properly defined [13]. For a fluid,

$$\varepsilon = 1 + B/2A \tag{3-6}$$

where B/A, the nonlinearity coefficient, is the constant coefficient of the first nonlinear term in the pressure density relation for an adiabatic medium.

Dissipation is included in the nonlinear analysis, as in the linear theory, by assuming the medium is viscous and heat-conducting. If terms of second order in smallness are retained in the initial equations of motion one obtains Burgers' equation presented here in the form [14]

$$u_x = (\varepsilon/c_o^2)uu_\tau + \alpha u_{\tau\tau}, \qquad (3\text{-}7)$$

where the subscripts represent partial derivatives with respect to x and τ. The constant α represents the medium dependent attenuation of the wave, assumed to have a quadratic frequency dependence.

The above equation describes an initially monochromatic, plane wave propagating in the positive x direction. Notice both the attenuation and nonlinear terms appear in the equation. The relative strength of the terms is reflected in the Gol'dberg number [14],

$$\Gamma = \varepsilon M_o/\alpha\lambda_o = 1/\alpha x_d, \qquad (3\text{-}8)$$

which is the nonlinear analogy to the acoustic Reynolds number, ($M_o = u_o/c_o$, the peak value of M). In the present study Γ is of unity order, therefore, both attenuation and nonlinearity play an important role and the Burgers' equation is used in the examination of ultrasonic waves by light diffraction.

A shock front forms because energy is passed from lower to higher spectral components of the wave. Since $\alpha = \alpha(w_o^n)$, $n \geq 1$, the dissipation is greater for higher frequency components, as a result, the discontinuity no longer completely develops and the wave is damped back into a semi-sinusoidal form.

Pulse Propagation and Reflection - Spectral Solution of Burgers' Equation:

A useful iterative, spectral solution to Burgers' equation considered here is similar to that given by Trivette and Van Buren [7] for the general case of plane, cylindrical and spherical finite amplitude waves, including arbitrary frequency dependent attenuation. Using a similar approach Haran and Cook [6] derive much the same algorithm as for the plane wave case of Trivett and Van Buren, differing only in notation. Ngoc et al. [15] combined the Haran and Cook model with an algorithm that treats nonspecular reflection of an ultrasonic beam from a solid

plate immersed in the liquid. Haran and Cook consider that the incremental change in the particle velocity u is approximated by a Taylor series expansion

$$u(x + dx,t) = u(x,t) + u_x dx \tag{3-9}$$

where quadratic and higher order terms have been neglected. For a general periodic wave, u is expanded in a Fourier series,

$$u = \sum_{n=-\infty}^{\infty} u_n \, e^{in(\tau + \beta_n)},$$

where u_n and β_n are the real amplitude and phase of the n^{th} Fourier spectral component. Since u and μ are proportional, the expansion is reexpressed as

$$u = \sum_{n=-\infty}^{\infty} U_n \, e^{in\tau}, \tag{3-10}$$

where $U_n = u_n \, e^{in\beta_n}$, is the complex amplitude.

The differential change of the n^{th} harmonic component is found by substituting above expression into Burgers' equation,

$$U_{nx} = (i\varepsilon w_o/c_o^2)\left(\sum_{j=1}^{n-1} jU_jU_{n-j} + \sum_{j=n}^{\infty} nU_jU^*_{j-n}\right) - \alpha n^2 U_n \tag{3-11}$$

where * indicates the complex conjugate. This form of the solution is well suited for computer calculation.

An examination of Eq. (3-11) provides insights into the mechanism of harmonic growth. The first summation expression represents the energy transfer between the lower harmonics and the n^{th} spectral component. The second sum is the energy exchange between the n^{th} and the higher order harmonics. This process can go in both directions depending on the relative phase

of each U_n. The full set of n equations are coupled.

To get the incremental change of each particle velocity component one substitutes Eq. (3-11) into Eq. (3-9) to obtain

$$U_n(x + dx) = U_n(x) + \{(i\varepsilon w_o/c_o^2)(\sum_{j=1}^{n-1} jU_jU_{n-j} + \sum_{j=n}^{\infty} nU_jU^*_{j-n}) - \alpha n^2 U_n\}dx. \qquad (3\text{-}12)$$

This expression is programmed into an iterative computer algorithm with specific restrictions on the size of the increment step, dx, and the number of terms retained in the infinite series. Calculational errors become sizable if dx is too large. If there are not enough terms retained in the Fourier expansion, then the last spectral term grows too large since it has no higher order terms to transfer its energy to.

The graphs a-f of Fig. 3-3 illustrate the wave time representation, and the corresponding set of Fourier amplitude spectra. The initial wave parameters for this example are f_o = 1 MHz and u_o = 0.1 m/s. For demonstration, the medium characteristics are B/A = 5.0, $\alpha(w_o^2)$ = 0.2 Np/m and c_o = 1500 m/s. Using these values in Eq. (3-5) yields x_d = 1.02 m. The summation is truncated to calculate 50 terms in the series and the propagation step is 0.5 % of the discontinuity distance.

Figure 3-3a depicts the wave at x = 0. The wave profile distortion at x = 0.5 m is apparent from Fig. 3-3b, as well as the harmonic growth. Figure 3-3c depicts the wave at $x = x_d$. The discontinuity is not completely formed due to the attenuation of the higher frequency components. At $x = 2x_d$ the sawtooth shape is completely formed, however, the dissipation prevents the wave profile from becoming nonphysical. The next two profiles are of the wave at $x = 10x_d$ and $20x_d$ where the wave has propagated into the "old age" region.

The spectral solution is easily adapted to pulsed wave propagation studies, provided the constraints of series truncation and propagation step size are observed. To demonstrate, the approximate pulse spectrum discussed in Section 2 is used as an

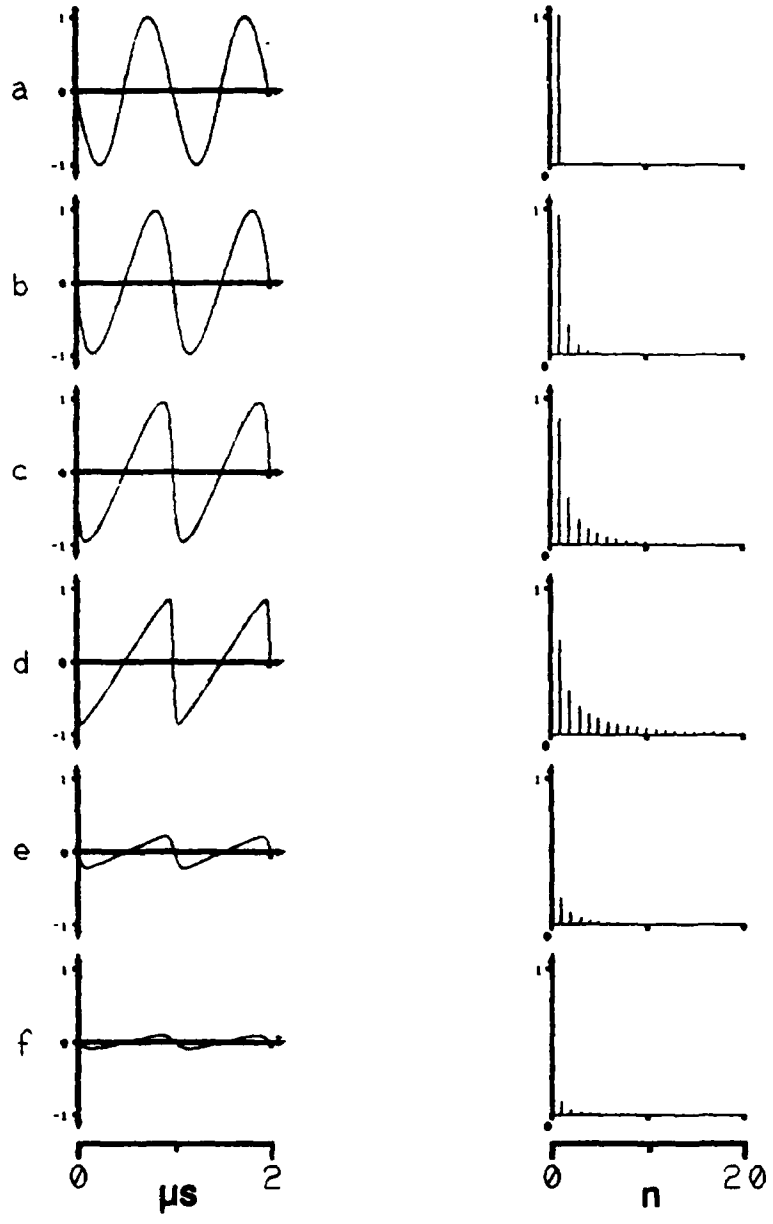

Fig. 3-3. Change of waveshape and corresponding Fourier frequency spectrum with increasing propagation distance in nonlinear medium, calculated for a continuous wave.

input to the propagation model as shown in Fig. 3-4.

Since any pulse spectrum initially has more than one spectral term the idea of a discontinuity distance loses meaning. The initial number of terms in a pulse spectrum is relatively large and thus limits the model to short propagation distances. Otherwise too many terms are needed in the spectrum to minimize computational errors.

The above set of figures show the pulse at propagation distance steps of 0.5 m. Although only the relevant number of terms are shown, the series was calculated to 120 terms and the distance step used was 5×10^{-4} m. Except for obvious amplitude drop from dissipation, the profile distortion in the time representation is subtle. Close examination reveals the shock front formation of each cycle within the pulse. The amplitude spectrum clearly demonstrates harmonic growth where the local peak values correspond to harmonics of the pulse center frequency, f_o.

The limitation of the model to short propagation distances, for pulsed waves, does not hamper the present investigation, since the apparatus limits actual pulse propagation to less than 0.5 m. A small amount of harmonic growth in the pulse spectrum produces obvious effects upon the shape of its light diffraction pattern. Various manifestations of this were investigated, a cross section of the results is given here.

Pulse Propagation and Reflection - Diffraction Pattern Experimental Results:

The first set of experiments was conducted for the situation where the maximum pulse amplitude remains the same while the travel distance of the pulses is increasing. Due to nonlinearities of the medium, the frequency spectrum of the pulses changes as the distance of propagation changes, which in turn causes changes in the calculated composition of the produced diffraction pattern - and evidently also changes in the observed light pattern. The following series of measured diffraction patterns, shown in Fig. 3-5, were produced by the ultrasonic source positioned, in the interaction vessel, from the light interaction

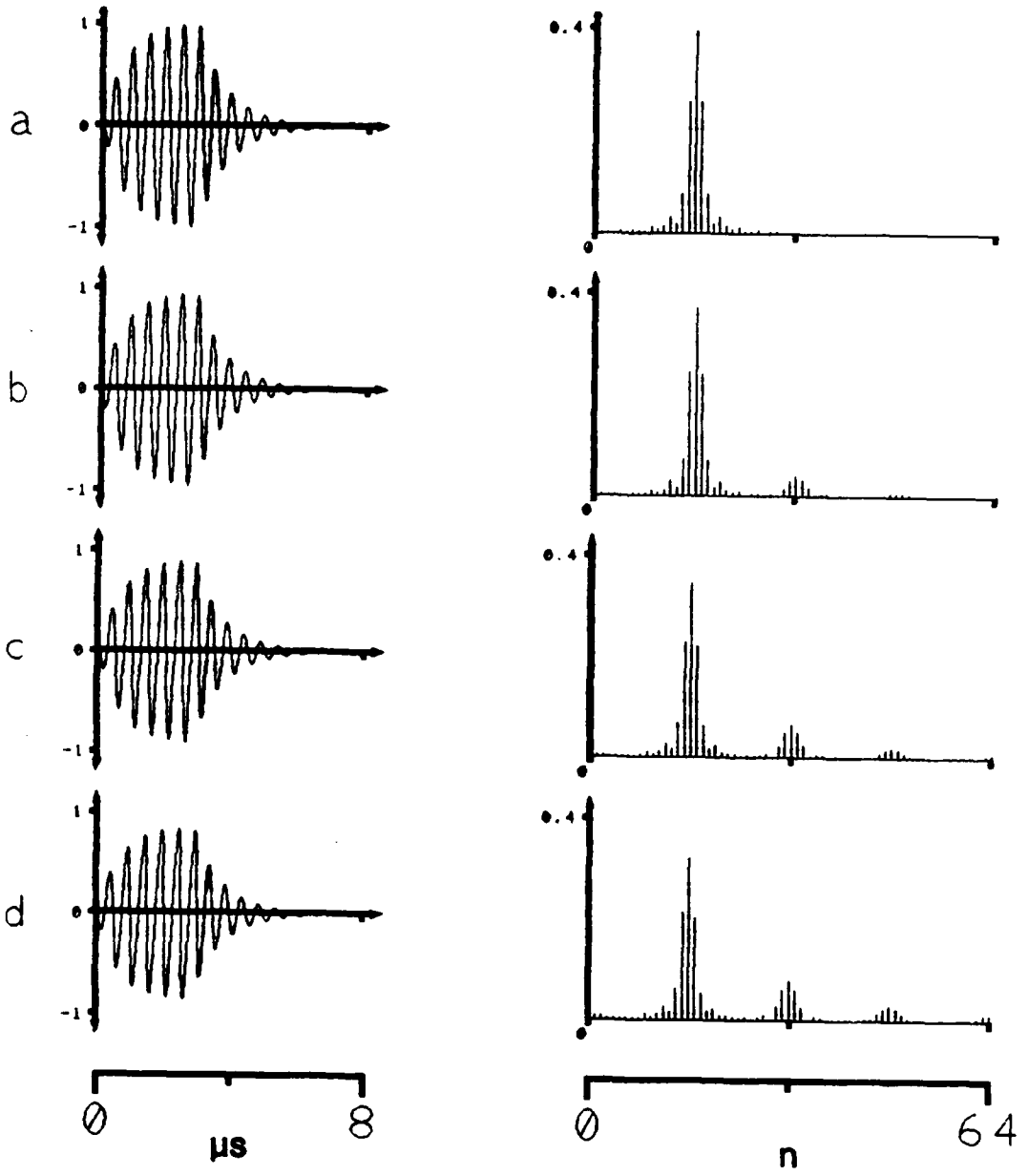

Fig. 3-4. Same as Fig. 3-3 but for a pulsed wave in a nonlinear medium.

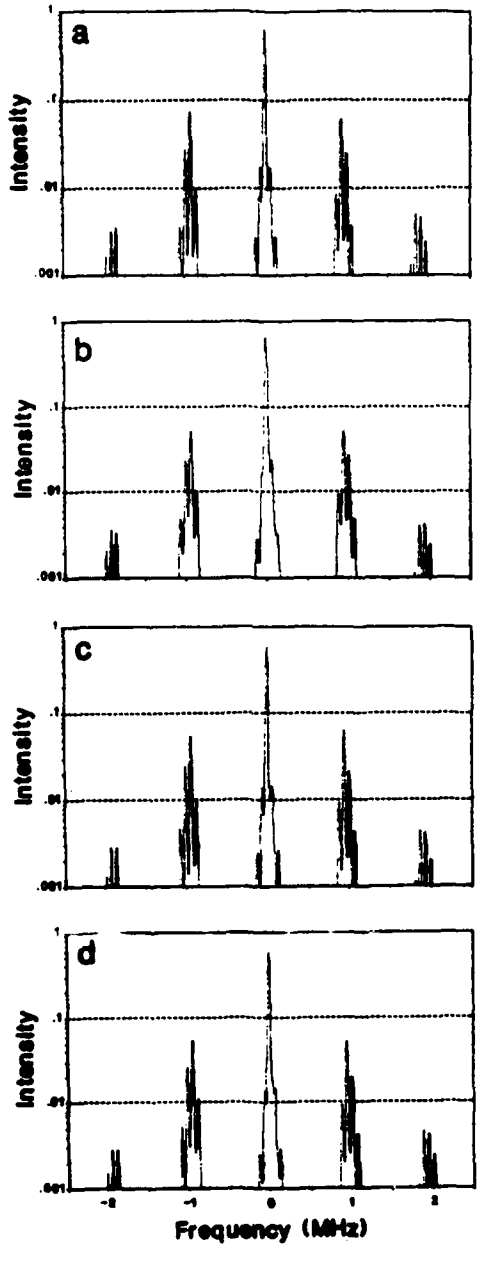

Fig. 3-5. Change in light diffraction pattern of pulsed wave as a function of propagation distance in a nonlinear medium.

region in steps of 10 cm. The normalized pulse spectrum used as input to the model is of the same configuration as the pulse described in detail in Sections 2. The Raman-Nath parameter is kept approximately constant, v = 1.35, for each stage of propagation.

The frequency spectrum of the output of the transducer (in response to an ideal electronic input signal - see previous sections) and the corresponding predicted light patterns are shown in Fig. 3-6.

The agreement between the measured and calculated patterns is consistent for all four patterns. They clearly demonstrate asymmetry resulting from nonlinear distortion of the pulse as a function of propagation distance in the medium, indicating that even a small amount of pulse harmonic distortion can produce a measurable change in the pulsed beam diffraction pattern.

The next set of light patterns were produced by a different input pulse configuration: f_p = 122.0 KHz, f_o = 0.987 MHz, burst = 3. In this configuration the pulse propagation distance was kept constant at 40 cm to the light beam interaction region. The pulse amplitude was changed, introducing increasing harmonic contributions. Figure 3-7 shows measured and theoretically determined diffraction patterns for different values of v.

Satisfactory agreement between prediction and measurement is indicated in all regions of the patterns. The asymmetry in the second set of measured satellite orders increases with input pulse amplitude as expected for finite amplitude waves.

The comparisons between measured and modelled diffraction patterns indicate that the original acousto-optically obtained transducer response model provides a satisfactory measure of the actual pulsed wave produced by the transducer in response to an ideal electronic excitation. The further agreement, seen in the propagated pulse patterns, verifies the propagation model.

The last portion of this section continues the verification of the theories and examines the result of probing a pulsed

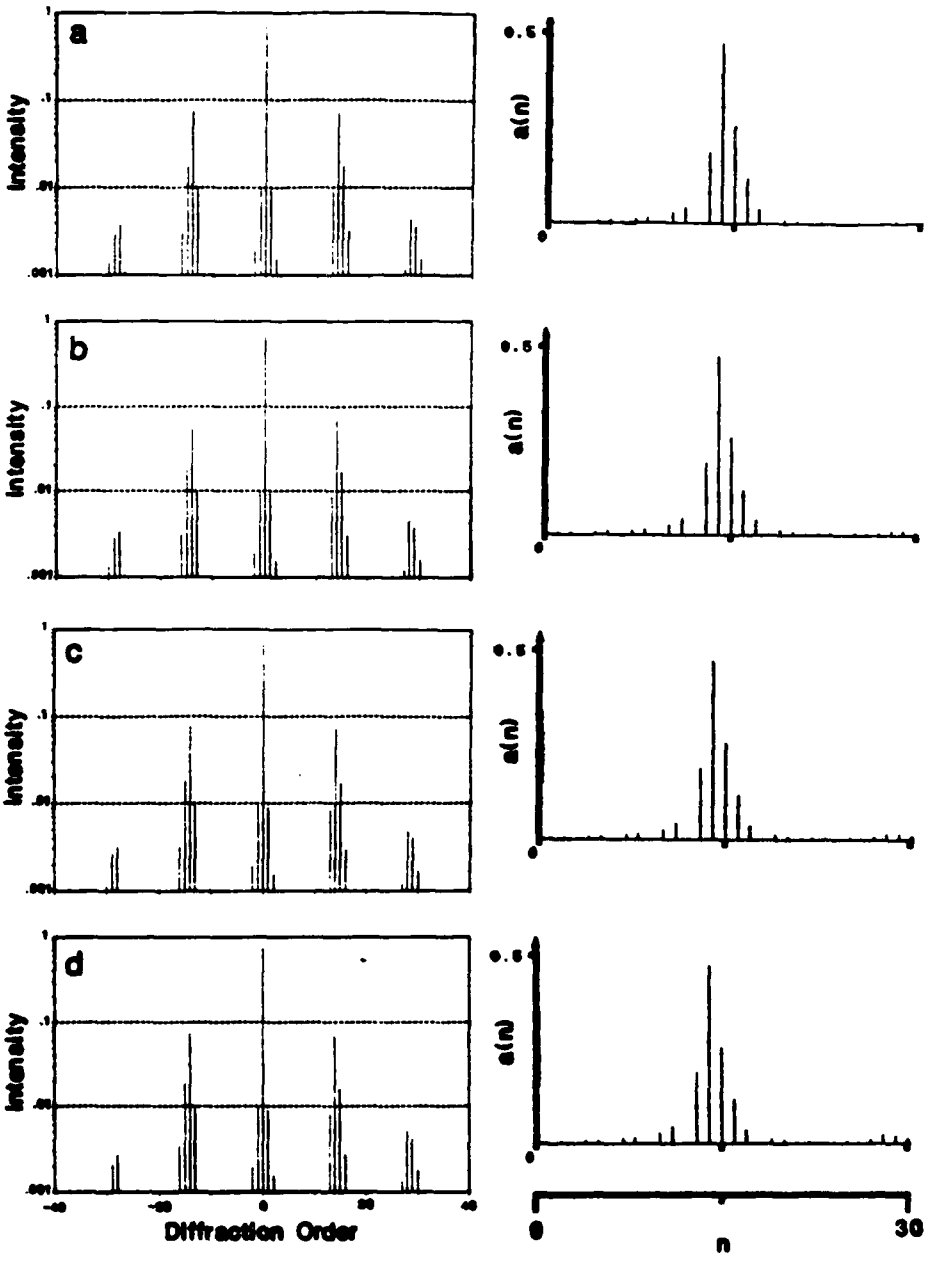

Fig. 3-6. Calculated diffraction pattern and Fourier frequency spectrum for the experimental cases shown in Fig. 3-5.

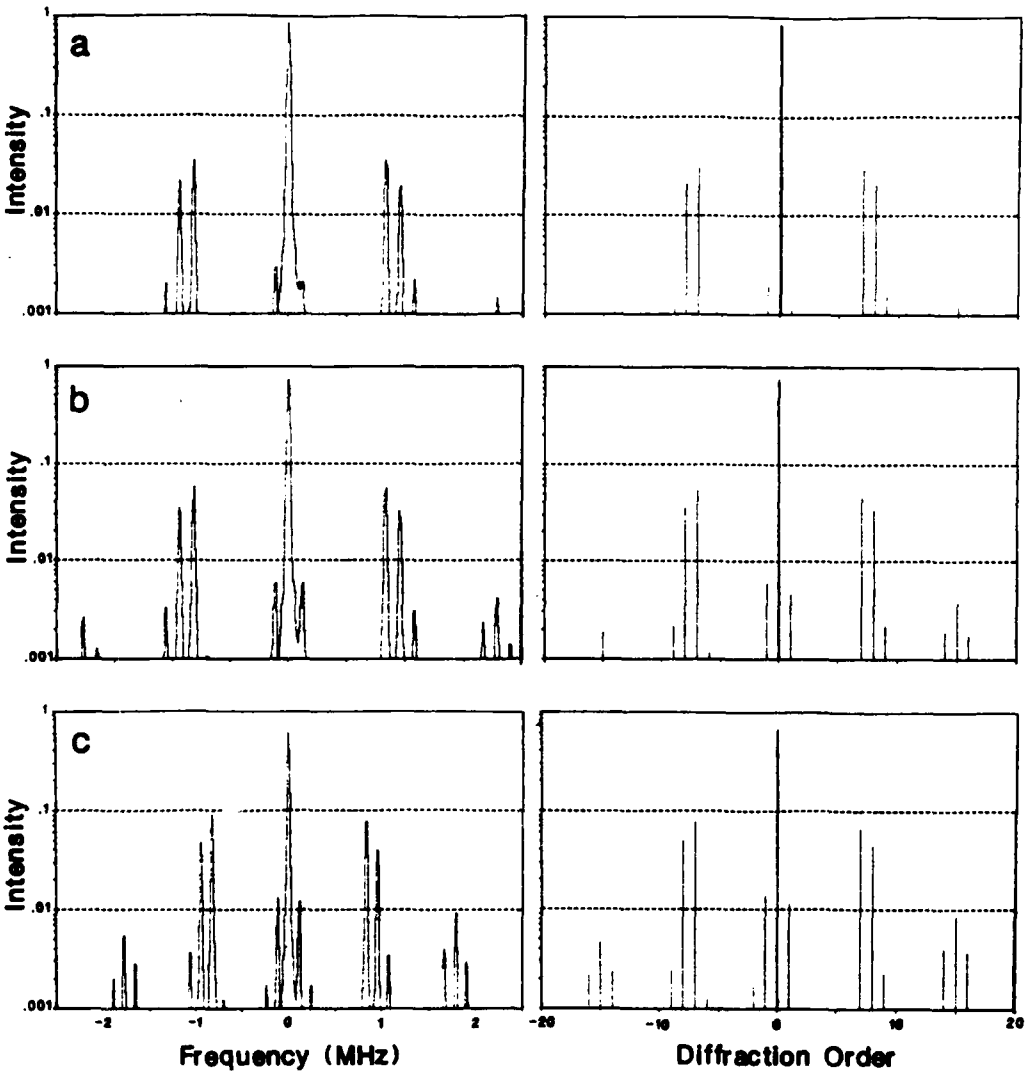

Fig. 3-7. Experimental and theoretical light diffraction pattern for pulses with increasing amplitude but fixed travel distance in nonlinear medium.

ultrasonic beam after it has interacted with a plate in the water.

Pulse Propagation and Reflection - Reflection Results:

This final portion of this section examines measured diffraction patterns produced by ultrasonic pulses which have been reflected from a brass plate immersed in the water. Initially, the reflection model is used with the propagation and diffraction models to show that measurements agree well with predictions of the theory.

A measured and a theoretically predicted diffraction pattern, shown in Fig. 3-8 was produced for a pulsed ultrasonic beam that has propagated 40 cm prior to interaction with the light beam and before it has been reflected by a brass plate. The pulse has repetition frequency of 132.2 KHz and center frequency of 0.925 MHz, burst of 2 and voltage input to the transducer of 150 mV producing a v = 1.45.

All the transducer response characteristics were again taken into consideration as had been the case for the previously described experiments. The predicted pattern agrees rather well with the measured light diffraction pattern. The apparent asymmetry, of the second set of satellite diffraction orders, represents nonlinear distortions due to the pulse propagating 40 cm.

A brass plate, of thickness D = 3.16 mm, is mounted, so that the propagation distance between the ultrasonic source and the plate is 11.5 cm, assuring that the total propagation distance, from source to light beam, is 40 cm.

The next set of diffraction patterns were produced by the ultrasonic beam after reflection from the brass plate. The reflected beam is properly directed into the interaction region while the angle of incidence of pulses against the flat plate is changed. The plate thickness and the pulse center frequency correspond to fD = 2.923 (MHz.mm). The patterns show results for incident angles, 25°, 28°, and 32° as read from the goniometer, through the A_1 mode of the brass plate. The predictions of the reflection, propagation and diffraction models are also shown for

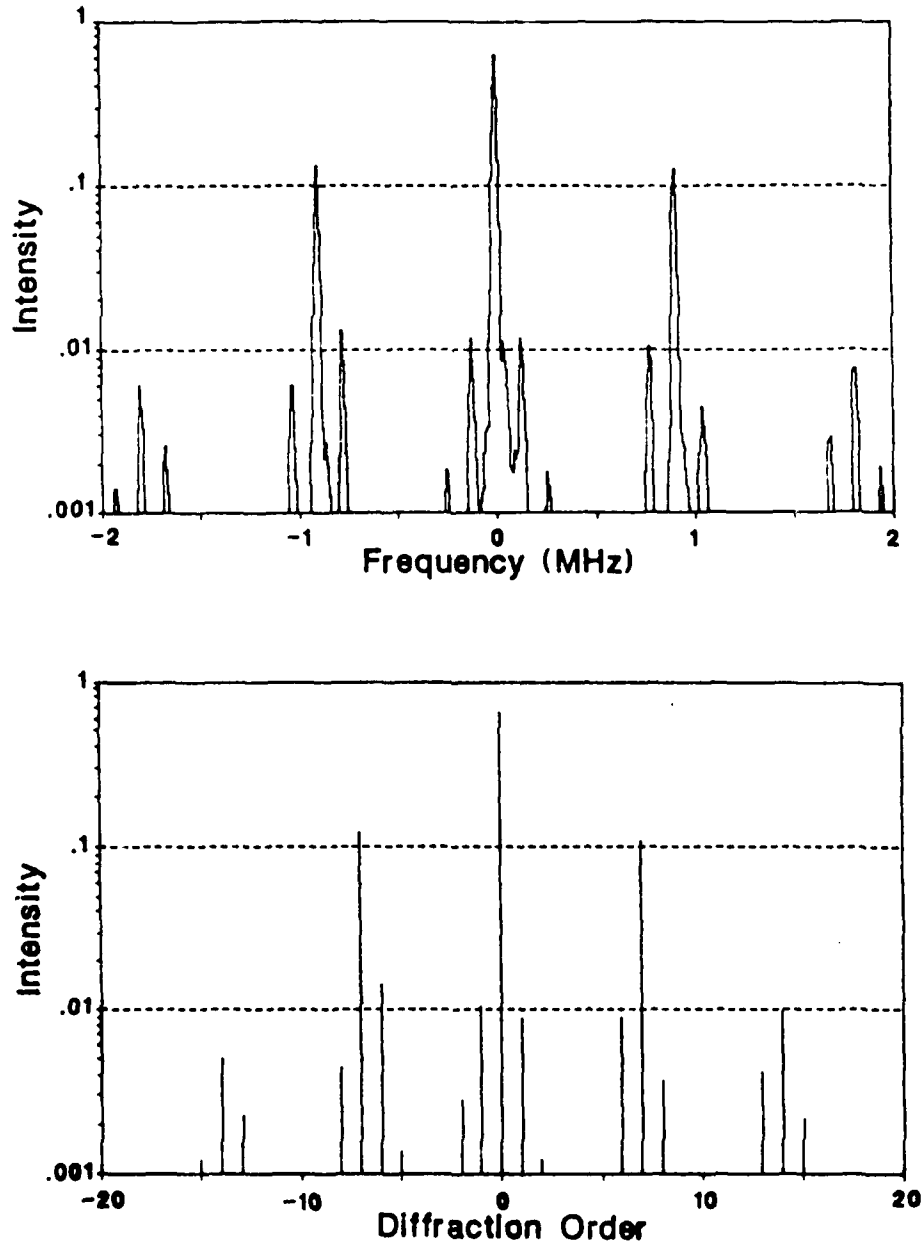

Fig. 3-8. Experimental (top) and theoretical (bottom) diffraction pattern for pulses after 40 cm travel but before reflection.

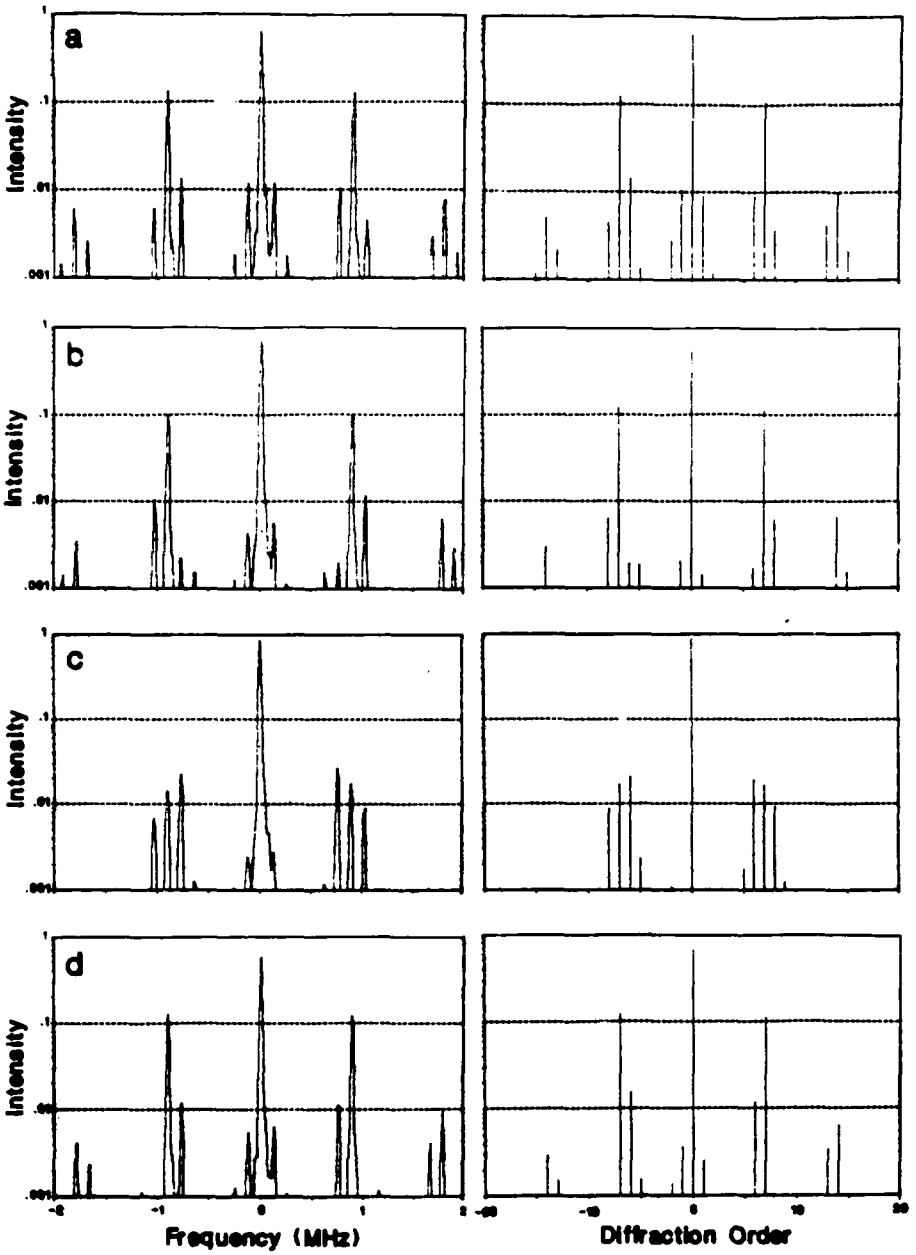

Fig. 3-9. Experimental (left) and theoretical (right) diffraction patterns after reflection, for different mode-angles of incidence.

each measured pattern as shown in Fig. 3-9. Each pattern indicates that the agreement between theory and experiment is again very good; moreover, it is obvious that different frequency terms has been filtered out of the pulse spectrum as the incident angle sweeps through the plate mode.

This, clearly can be used as a mechanical frequency filter, and this issue is discussed in the last section of this Report.

REFERENCES

[1] A.L. Van Buren, J. Acoust. Soc. Am. 44, 1021 (1968).

[2] M.A. Breazeale, L. Adler and L. Flax, J. Acoust. Soc. Am. 56, 866 (1974).

[3] M.A. Breazeale, L. Adler and J.H. Smith, Sov. Phys. Acoust. 21, 1 (1975).

[4] M.A. Breazeale, L. Adler and G.W. Scott, J. Appl. Phys. 48, 530 (1977).

[5] O.V. Rudenko and S.I. Soluyan, **Theoretical Foundations of Nonlinear Acoustics**, Plenum, New York (1977).

[6] M.E. Haran and B.D. Cook, J. Acoust. Soc. Am. 73, 774 (1983).

[7] D.H. Trivett and A.L. Van Buren, J. Acoust. Soc. Am. 69, 953 (1981).

[8] H.L. Bertoni and T. Tamir, Appl. Phys. 2, 157 (1973).

[9] T.D.K. Ngoc and W.G. Mayer, IEEE Trans. Sonics Ultrason. SU-27, 229 (1980).

[10] J.M. Claeys and O.J. Leroy, J. Acoust. Soc. Am. 72, 585 (1982).

[11] M. Rousseau and Ph. Gatignol, J. Acoust. Soc. Am. 78, 1859 (1985).

[12] K.R. King, "Propagation and Reflection of a Finite Amplitude Ultrasonic Beam Including Harmonic Content - A Numeric Model," Ph.D. Thesis, Georgetown University (1983).

[13] R. T. Beyer, J. Acoust. Soc. Am. 32, 719 (1960).

[14] D. T. Blackstock, J. Acoust. Soc. Am. 36, 534 (1964).

[15] T. D. K. Ngoc, K. R. King, and W. G. Mayer, J. Acoust. Soc. Am. 81, 874 (1987).

Section 4

SPECTRAL FILTERING AND NEGATIVE GROUP VELOCITY

A. SPECTRAL FILTERING

Thin metal plates immersed in water can be used to selectively transmit ultrasonic waves of given frequencies, depending on the angle of incidence of the wave onto the metal plate. Based on this principle, a spectral filter for demonstrating the presence of second harmonics in a continuous, finite amplitude wave was used by Zankel and Hiedemann [1]. However, at that time the interpretation of the observed effect was purely qualitative. The results presented here are based on quantitative calculations which consider the mode structure of a metal plate [2] (i.e., the Lamb wave velocity dispersion), the angular dependence of the coefficient of reflection of a plane wave from a plate as a function of frequency [3], and the relation of mode structure and reflection [4]; the analysis is made for ultrasonic pulses where the influence of nonlinear processes on the frequency contents of the pulse has been taken into account [5] on the basis of a numerical solution [6] of the plane wave Burgers' equation.

Pulse and Reflector Description

A schematic diagram of the system to be analyzed is shown in Fig. 4-1. An ultrasonic pulse traveling in water, containing 20 wave trains of frequency 2 MHz, is incident at an angle Θ on a flat brass plate. The assumed initial pulse shape is shown in the figure. The pulse repetition rate is 100 kHz.

With these assumptions one can now perform a spectral analysis of the pulse sequence. The lowest frequency component is the repeat frequency of 100 kHz. The number of frequency components (multiples of 100 kHz) carried in all subsequent calculations for pulse propagation in the nonlinear medium and reflection at the plate was 120. This is a sufficient number to describe and reconstruct the pulse at any location along its path.

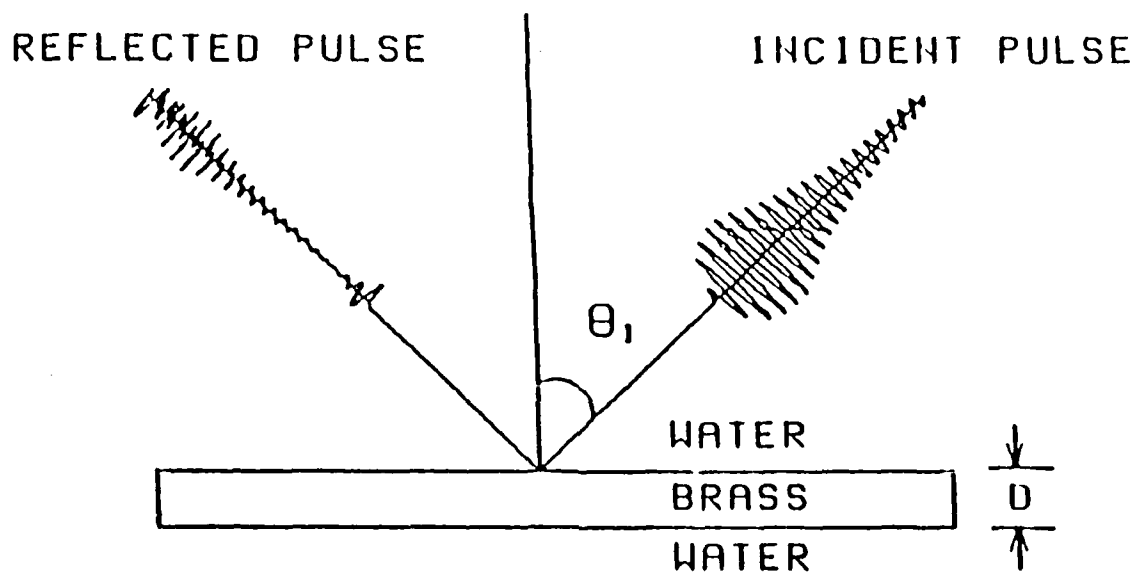

Fig. 4-1. Schematic diagram of system to be analyzed.

The changes in pulse shape and spectral contents caused by reflection from the metal plate depend on the amount of harmonics present when the pulse arrives at the plate, the product ultrasonic frequency times plate thickness (fd), the incidence angle (θ) as well as the amplitude and phase of the reflection coefficient as a function of θ and fd.

A typical reflection coefficient graph for a brass plate in water is shown in Fig. 4-2. For given values of velocities, density, and an fd of 2.5 MHz.mm, one notes that there are four angles of incidence where the reflection coefficient is essentially zero. These angles, 6.6, 23.75, 44.15, and 48.45 degrees, represent resonance conditions at which the S_1, A_1, S_0, and A_0 Lamb modes are excited and reflection is minimal.

It should be noted that the angle of zero reflection is different for every frequency component contained in an ultrasonic pulse that has propagated through a nonlinear medium. Thus phase and the modulus of reflection must be known for all frequencies in a pulse if one expects to predict the changes of pulse shape introduced by reflection from a plate.

It is perhaps evident that, in general, the angle of total transmission for a certain frequency f may well be the angle for total reflection for frequency 2f - this having been the assumption made by Zankel and Hiedemann [1]. This, however, is not necessarily true in all cases, particularly when the angle of incidence is selected to fall between two closely spaced modes, as for instance at 46.5 degrees for the conditions described in Fig. 4-2. Reflection is not total at this angle, and it can be shown that the phase shift upon reflection is neither 0 nor π. This introduces more complications into the prediction of the reflected finite-amplitude pulse shape than into the determination of the events when the angle of incidence is directly at or far away from a mode (0% or 100% reflection). Therefore, calculations were made to illustrate the changes in frequency components of a reflected pulse.

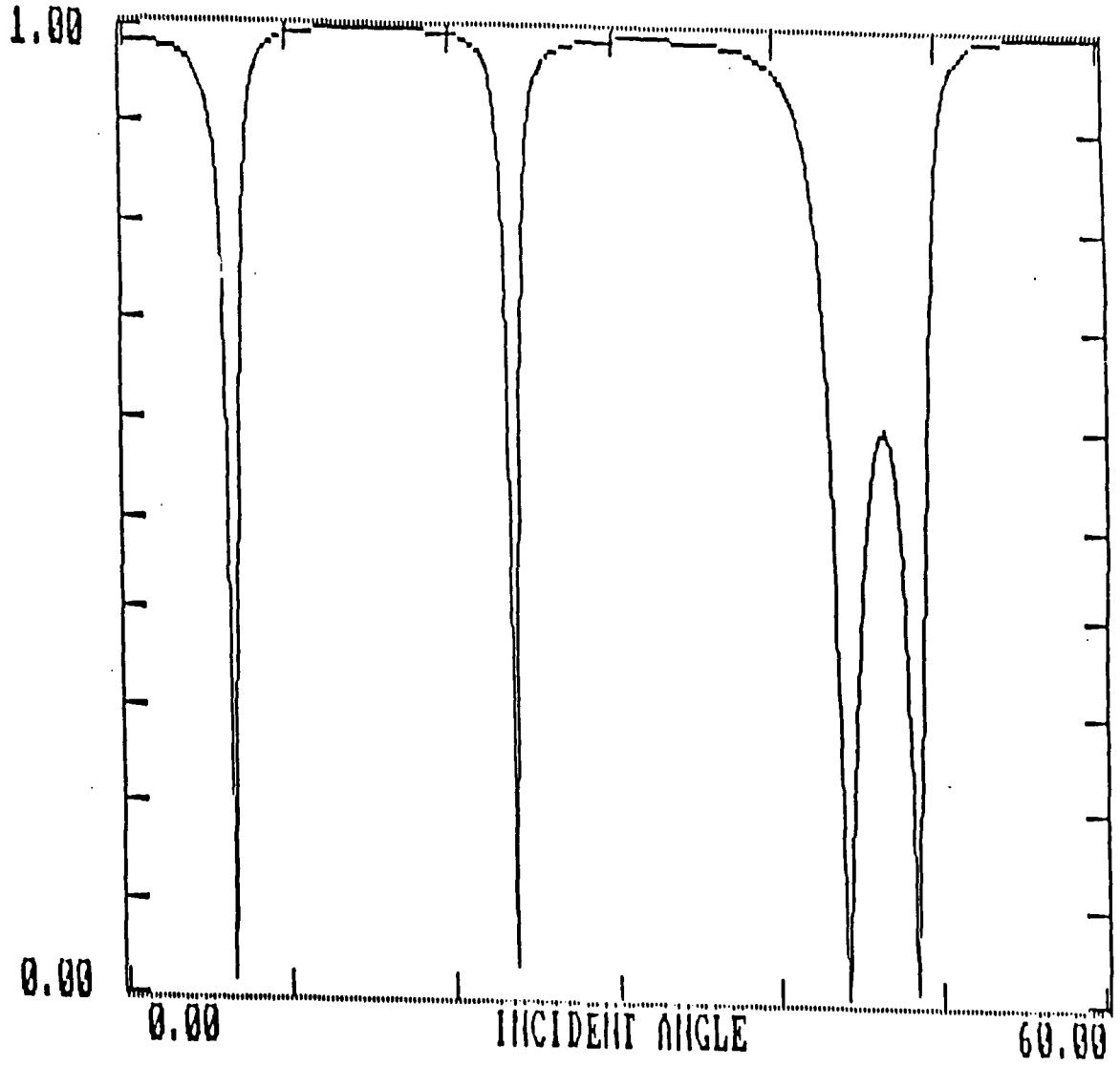

Fig. 4-2. Reflection coefficient for a brass plate in water.

Calculations and Results

The calculations start with the determination of the frequency spectrum of the assumed pulse shape as described above. This initial pulse is shown in Fig. 4-3a which can be transformed into a spectral representation as shown in Fig. 4-4a where the strongest component corresponds to the 2 MHz modulation frequency of the pulse and the other components shown differ by 100 kHz, the assumed repetition frequency of the pulse sequence.

As the pulse travels through the nonlinear liquid, its spectral composition changes; these changes are calculated using a technique described by Neighbors et al [7,5]. This calculation shows the expected result that a second harmonic frequency component appears in the pulse, together with 100 kHz repetition rate frequency components centered around the 4 MHz second harmonic, as shown in Fig. 4-4b. Having carried the calculation to 120 frequency components, one can use this spectrum to construct the waveshape: this is shown in Fig. 4-3b. The expected saw-tooth nature of the waveshape within the pulse can be noted.

The remainder of Figs. 4-3 and 4-4 refer to the waveshapes after reflection. The reflection after a 40 degree incidence (far away from a Lamb mode excitation situation, see Fig. 4-2) shows that relatively little was changed in the spectral composition during the reflection process, as depicted in Figs. 4-3c and 4-4c. The waveshape and the spectral composition differ very little from those shown in Figs. 4-3b and 4-4b. But when the incident pulse impinges at a Lamb angle, as shown for a 44.15 degree incidence in Fig. 4-4d, the 2 MHz component disappears from the spectrum because the reflection amplitude for that case is zero - while the reflection coefficient amplitude for the second harmonic at that angle is close to total. The result is, as Fig. 4-4d and the reconstruction of the waveshape shown in Fig. 4-3d show, that the pulse modulation frequency is primarily 4 MHz after reflection.

The final set of results in Figs. 4-3 and 4-4 show that reflection at an angle which is close to two distinct modes introduces non-total reflection of the fundamental as well as a

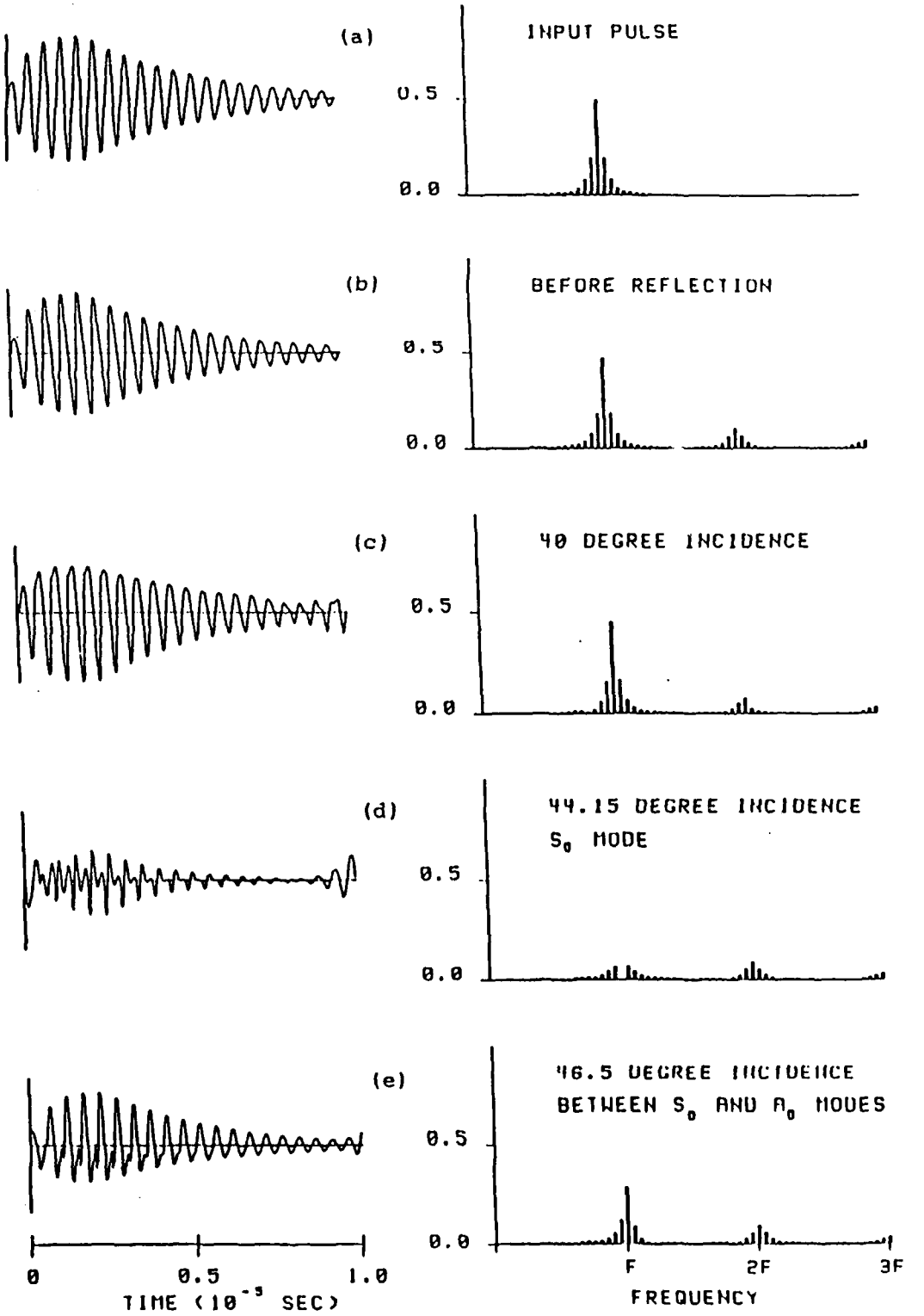

Figs. 4-3 and 4-4. Pulse shapes and frequency components before and after reflection from brass plate, showing frequency filtering for some angles.

phase shift which results in a rather complicated addition of pulse changes caused by the influence of the two adjacent modes.

B. NEGATIVE GROUP VELOCITY

It has been established theoretically that a certain propagation mode of Lamb waves exhibits a negative group velocity for a particular range of fd, where f is the ultrasonic frequency and d is the plate thickness. The present paper demonstrates experimental evidence for the existence of such a propagation characteristic. Observations of negative group velocity for Lamb waves were made on a brass plate immersed in water in the fd range of 2.05 - 2.30 MHz-mm for the A_1 and S_1 modes. The measured values of phase and group velocities were compared to theoretical values for the cases under consideration. The observed signal amplitude is discussed in the light of possible noise factors.

Introduction

The phase velocity of a Lamb wave propagating along the interface between a solid plate and a liquid like water depends not only on the type of solid but also on the frequency of the Lamb wave, f, and on the thickness of the plate, d. Plotting the phase velocities of the various modes as function of the product fd results in the so-called velocity dispersion curves. Defining a phase velocity, in the most general terms, as Ω/k and noting that this quantity is not a constant, then there will be another set of velocities, defined in the most general terms as the values of $d\Omega/dk$, which results in a family of curves depicting the group velocities.

The numerical values of the phase velocities of Lamb modes are usually quite different from the values of the group velocities. The slope of the phase velocity dispersion curves is such that almost all corresponding group velocities are positive, implying that the energy flow direction and the direction of the phase velocity are the same.

In general, the group velocity of a given Lamb mode can be calculated when the set of phase velocity dispersion curves is known. The phase velocity dispersion curves can be calculated by various standard methods, and the appropriate differentiation of the resulting curves leads to the numerical values of the group velocities. It was predicted by Tolstoy and Ustin [8] that the group velocity may have a negative value in a narrow range of fd, and it was shown by Biot [9] that the group velocity is identical to the velocity of energy transport in a dispersive medium.

The implications are that phase and energy propagate in opposite directions when the group velocity of a given mode assumes a negative value. The range of parameters where this may occur is rather limited. This paper illustrates an experimental technique which allows one to measure the numerical values of negative group velocities of Lamb waves directly. Comparisons of theoretical values of group velocities and experimentally obtained results are given, establishing the fact that Lamb waves may indeed travel with negative group velocities.

Predictions

A 1.04 mm thick brass plate was used in the experiments. The phase velocity dispersion curves for this plate are shown in Fig. 4-5. This figure shows both the symmetric and antisymmetric modes of vibration, indicating that, e.g., this brass plate can support five different modes when the frequency of excitation is such that the product frequency (in MHz) times plate thickness (in mm) is 3. The phase velocity of these possible modes would be determined by the five possible solutions to the defining Lamb wave equations.

Rather than using the values of the phase velocity as the parameter for the ordinate in Fig. 4-5, the critical angle (in degrees) is used. This angle refers to the incident angle of an ultrasonic wave striking the plate, as indicated in Fig. 4-6. From the most general form of Snell's law

$$\sin\theta_i/v_i = \sin\theta_j/v_j$$

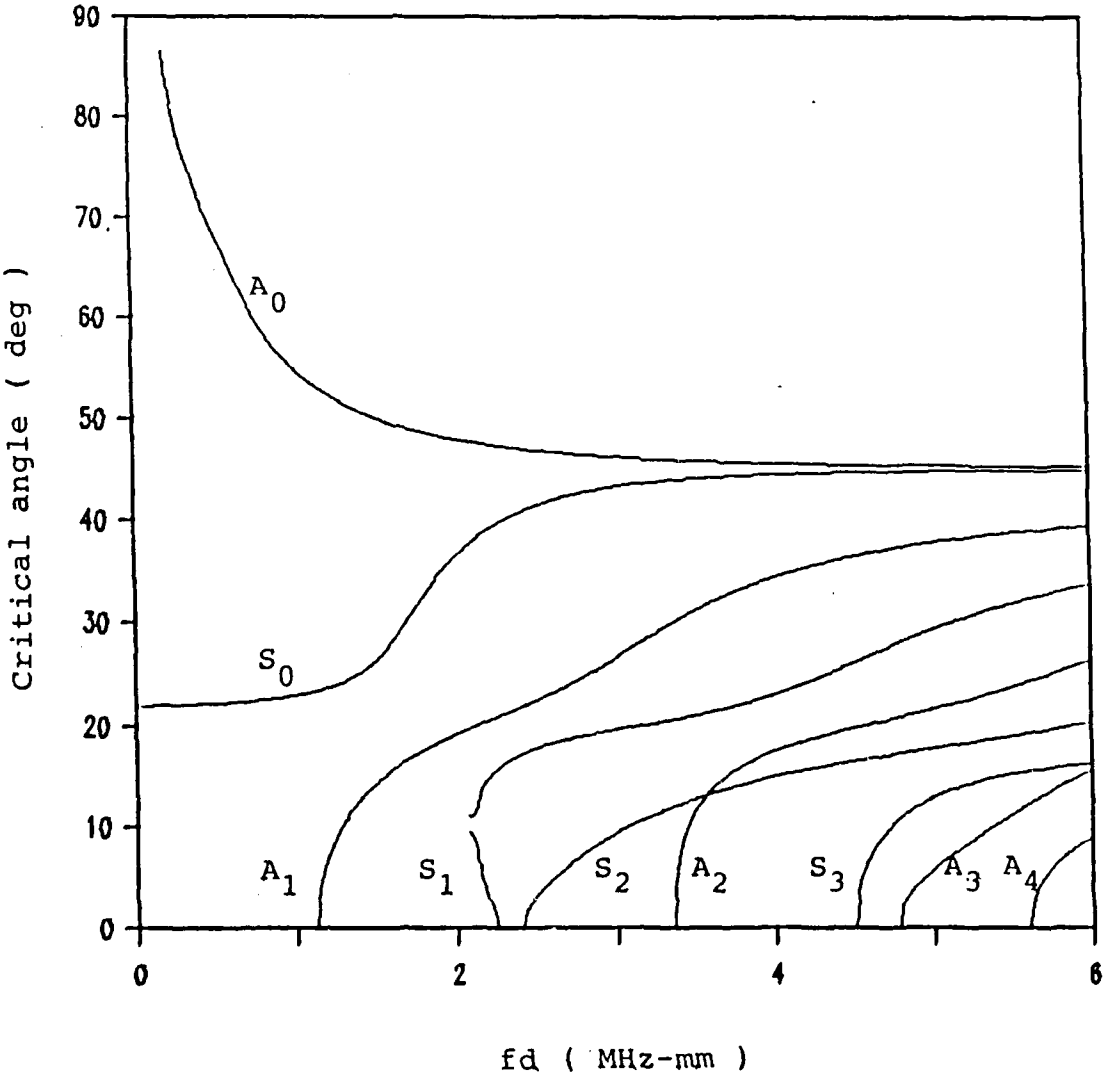

Fig. 4-5. Critical angle dispersion curves for brass plate in water.

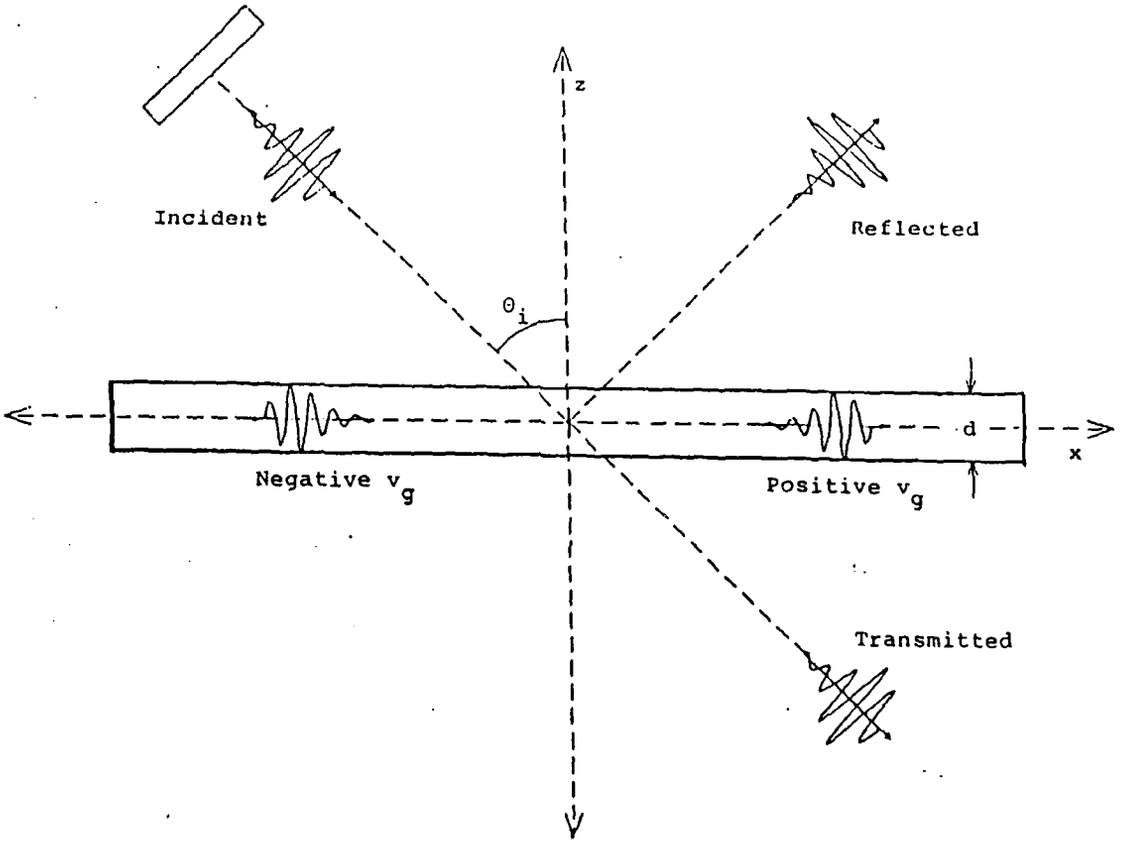

Fig. 4-6. Diagram of directions of pulse propagation.

one can easily see that there will be one specific angle of incidence Θ_i in the liquid, where the sound velocity is v_i, which will generate a wave with phase velocity v_j, propagating along the surface such that $\sin\theta_j = 1$. Any one of these "Lamb angles" or critical angles corresponds to the phase velocity of a possible mode.

One notes that all velocity dispersion curves in Fig. 4-5 have a slope which is either positive or negative for all values of fd, except the S_1 curve. It is double-valued in the fd-range from about 2.0 to 2.3, and it changes its slope in this range. This implies, theoretically, that the numerical value of the group velocity must change from positive to negative in this narrow range [2,8,9].

The corresponding values of the group velocities of the Lamb modes are indicated in Fig. 4-7. One notes that all values are positive except one rather narrow section of the S_1 curve. Negishi [10] reported some evidence of this phenomenon in an aluminum plate. He interpreted the observed events as being related to nonspecular reflection of a bounded ultrasonic beam whereby the trailing field reversed its position with respect to the specularly reflected field, indicating that the Lamb wave is propagating in the opposite direction.

Experimental Procedure

A diagram of the experimental apparatus used is shown in Fig. 4-8. A PZT 2-MHz transducer is mounted on a goniometer so that the incidence angle at the brass plate can be varied. The whole assembly is immersed in a water tank. The transducer is driven in a pulsed mode and any ultrasonic energy which is converted to a plate mode traveling with either positive or negative group velocity (see Fig. 4-6) can be monitored by means of two miniature hydrophones whose sensitive areas can be brought in contact with the surface of the brass plate.

The two probes can be moved along the plate so that the distance from the center of the incident pulse on the plate to

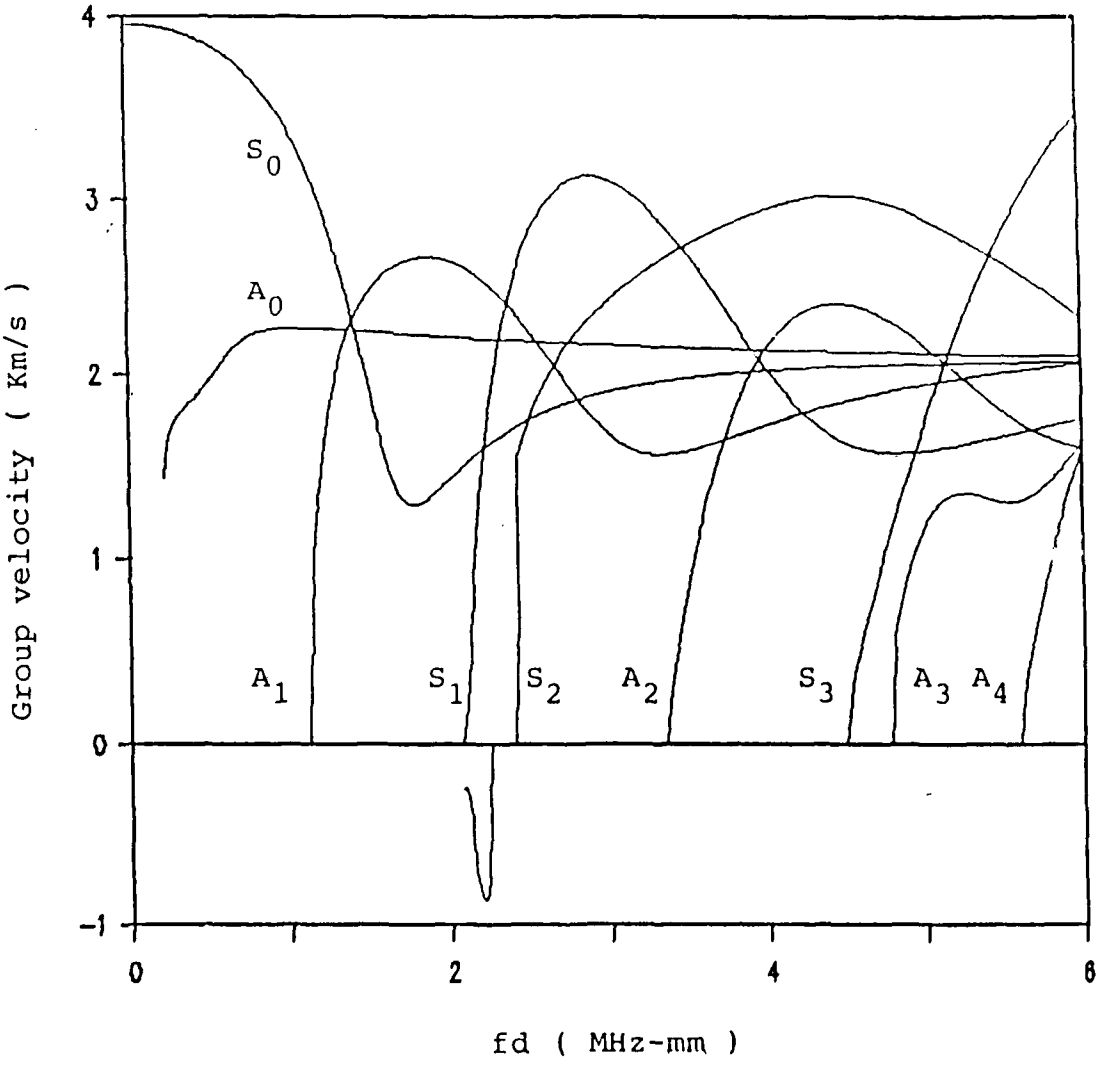

Fig. 4-7. Group velicies of Lamb modes for brass plate in water.

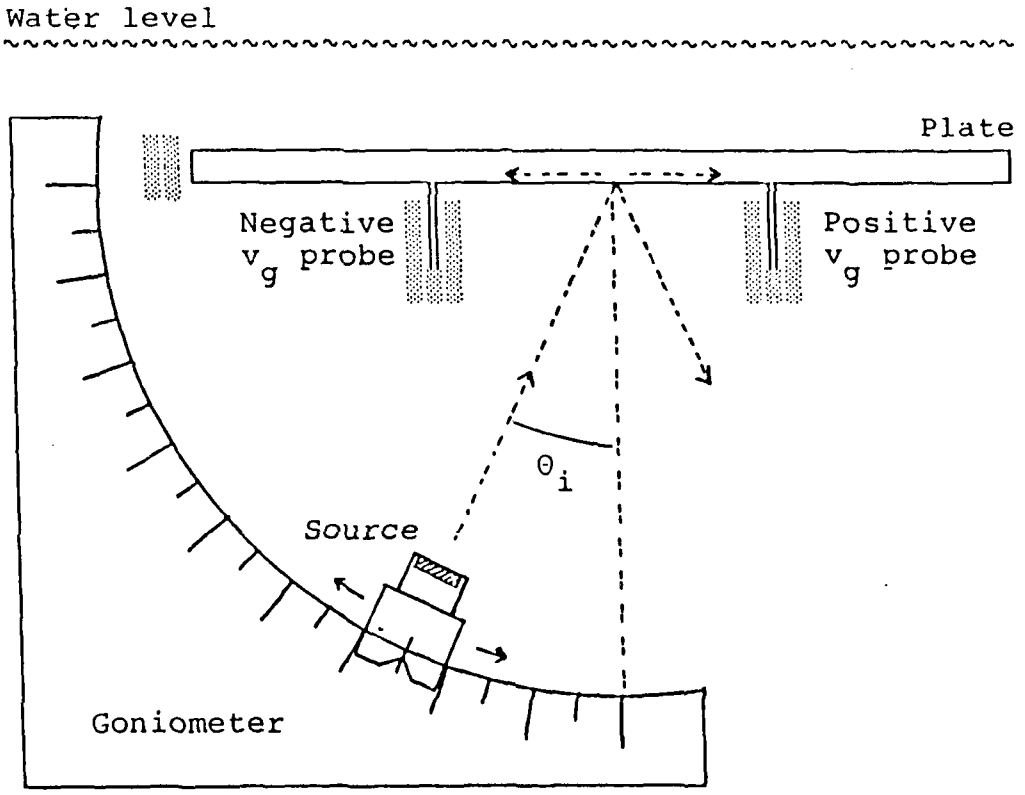

Fig. 4-8 Schematic diagram of experimental arrangement used.

the measurement point can be changed, allowing for multiple measurements of the velocity with which the energy of the Lamb mode travels along the plate. Absorbing material is used throughout to suppress any spurious reflections in the water tank.

The electrical output of the two hydrophone probes is amplified and displayed on oscilloscopes together with the pulse that drives the transducer. The repetition rate is kept low to assure that possible reflections will no longer be recorded by the probes before a new pulse is generated. The selective response of the two probes and pulse travel times yield both magnitude and sign of the group velocity.

The experiment is conducted by setting the frequency to a value which, in combination with the thickness of the brass plate, makes the value of fd in the vicinity of 2.1. The incident angle is changed until a plate mode is set up. The location of the probes is then changed by approximately 10 mm along the energy flow axis and a new time delay reading is taken.

Results

In order to be able to compare measured and theoretical values of group velocities one should first compare the theoretically determined phase velocity dispersion curves and the experimentally measured critical angles (the "Lamb angles"). This is essential since deviations between calculated and measured phase velocity curves will certainly result in serious disagreements of theory and measurement for the group velocity curves, considering that the latter are obtained by differentiation of the former.

To show the level of agreement for both cases, results are included in Fig. 4-9 for the A_1 and the S_1 modes for the fd-range of interest. It should be noted that the A_1 mode is not expected to show a change in slope, thus no change in the direction of energy transport will be expected when that mode is excited. Nevertheless, the data for that mode are included as a reference of the general agreement of theory and experimental measurements.

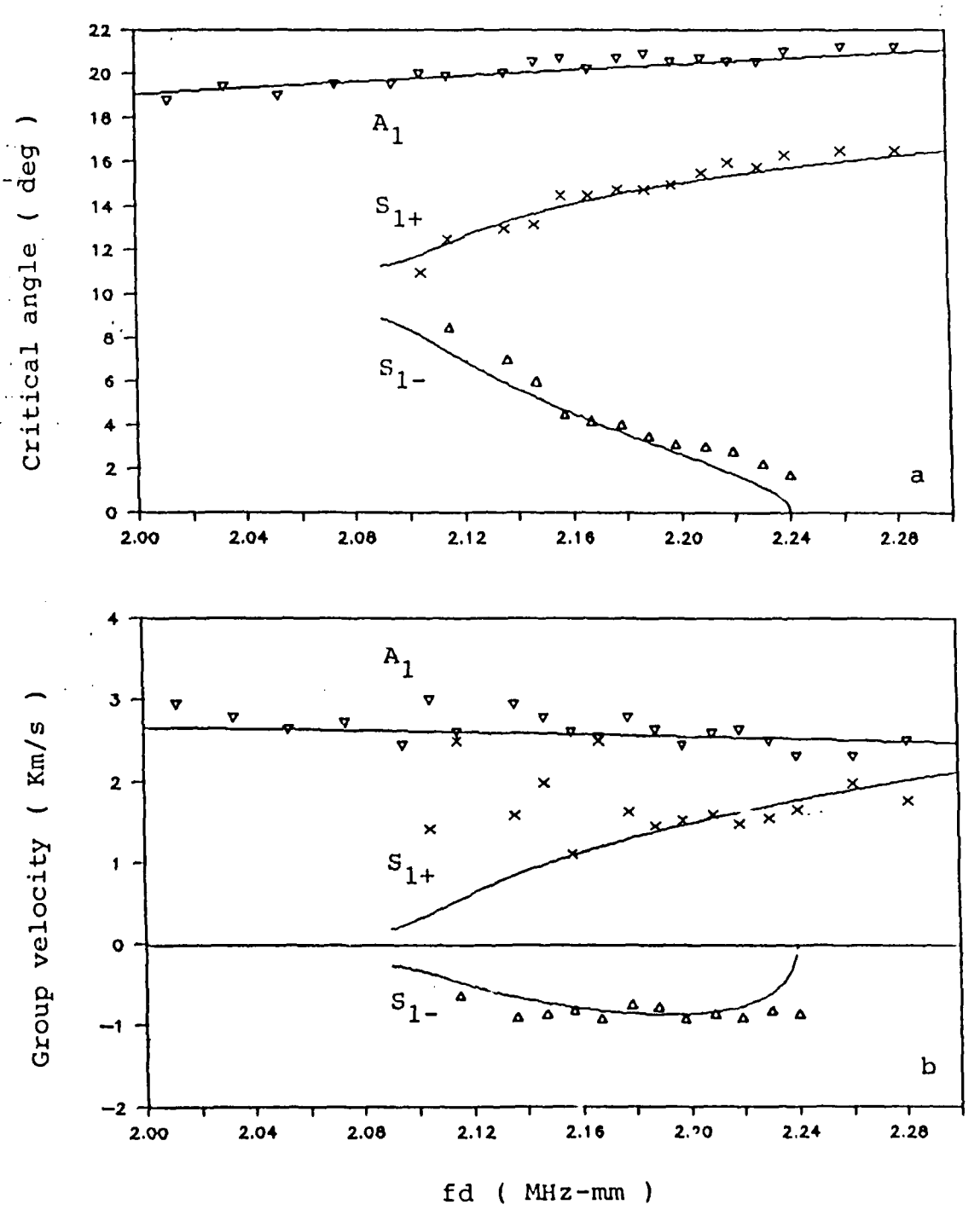

Fig. 4-9. Experimental points and theoretical curves for (a) the phase velocity, expressed as critical angle, and (b) the group velocity in the vicinity of critical fd-range.

Figure 4-9a shows the experimental confirmation of the calculated values for the critical angles (phase velocity); it is an enlargement of a very small section of Fig. 4-5 where now the S_1 curve has been divided into a positive and a negative section to indicate the sign of the group velocity.

Figure 4-9b shows the corresponding measurements of the group velocities for the two modes in the fd-range of interest. The agreement is reasonable for most of the range considered. A reliable measurement of the group velocity becomes rather difficult when the value of the velocity approaches zero which is the case when the slope of the dispersion curve changes from positive to negative.

But in general, the results presented here do confirm the theoretical prediction that Lamb waves with negative group velocities do exist, i.e., modes exist where phase and group velocities are in opposite directions. In addition, it has been observed that the mode becomes highly attenuated when its group velocity becomes very small.

REFERENCES

1. K.L. Zankel and E.A. Hiedemann, J. Acoust. Soc. Am. **30**, 582 (1958).
2. I.A. Viktorov, Rayleigh and Lamb Waves, Plenum Press, New York, 1967.
3. L.E. Pitts et al, IEEE-Trans. SU, **SU-24**, 101 (1977).
4. T.D.K. Ngoc and W.G. Mayer, IEEE-Trans. SU, **SU-29**, 112 (1982).
5. T.H. Neighbors and W.G. Mayer, J. Acoust. Soc. Am. **74**, 146 (1983).
6. M.E. Haran and B.D. Cook, J. Acoust. Soc. Am. **73**, 774 (1983).
7. W.G. Mayer and T.H. Neighbors, Ultrasonics **25**, 83 (1987).
8. I. Tolstoy and E. Usdin, J. Acoust. Soc. Am. **29**, 37 (1957).
9. M.A. Biot, Phys. Rev. **105**, 1129 (1957).
10. K. Negishi, J. Acoust. Soc. Am. **64**, S63 (1978).

ONR-SPONSORED PAPERS PUBLISHED DURING CONTRACT PERIOD 1985-1988

W. G. Mayer, Ultrasonic reflection and material evaluation, Rev. Physique Appl. 20, 377-81 (1985).

W. G. Mayer, Principles of acousto-optic techniques, Proc. Ultras. Int'l. 10, 170-174 (1985).

W. G. Mayer, Non-invasive method of measuring acoustic fields, Proc. South African Acoust. Congr. 1, 136-49 (1985).

W. G. Mayer, Acousto-optic imaging of scale model underwater sound fields, Proc. South African Acoust. Congr. 1, 240-46 (1985).

D. E. Himberger, G. I. Malinin, and W. G. Mayer, A low temperature acoustic system for inducing nonthermal ultrasonic damage in biological targets, Rev. Sci. Instrum. 57, 1681-83 (1986).

T. H. Neighbors and W. G. Mayer, Ultrasonic pulse shape deformation observation through optical probing, Proc. 12 ICA, 2, G7-4 (1986).

W. G. Mayer and T. H. Neighbors, Acousto-optic ultrasonic pulse characterization, Ultrasonics 25, 83-86 (1987).

T. D. K. Ngoc, K. R. King, and W. G. Mayer, Numerical model for nonlinear and attenuative propagation and reflection of an ultrasonic bounded beam, J. Acoust. Soc. Am. 81, 874-80 (1987).

W. G. Mayer, **Anisotropic material evaluation with ultrasonics.** In "Ultrasonic Methods in Evaluation of Inhomogeneous Materials", NATO ASI Series, Applied Sciences 126, 3-11 (1987).

T. D. K. Ngoc, K. W. Ng, and W. G. Mayer, Feature mapping of Y-shaped cracks using ray tracing interpretation, Ultrasonics 25, 215-20 (1987).

W. G. Mayer, T. D. K. Ngoc, and J. Wolf, Experimental verification of Lamb waves propagating with a negative group velocity, Ultrasonic International, Conf. Proc. 447-51 (1987).

J. Wolf, T. D. K. Ngoc, R. Kille, and W. G. Mayer, Investigation of Lamb waves having negative group velocity, J. Acoust. Soc. Am. 83, 122-26 (1988).